FINAL REPORT ON APPLIED BEYOND 5G TECHNOLOGIES

Deliverable D6.5

Co-funded by the European Union

6GSNS

The TARGET-X project has received funding from the Smart Networks and Services Joint Undertaking (SNS JU) under the European Union's Horizon Europe research and innovation programme under Grant Agreement No: 101096614

FINAL REPORT ON APPLIED BEYOND 5G TECHNOLOGIES

GRANT AGREEMENT	101096614
PROJECT TITLE	Trial Platform foR 5G EvoluTion – Cross-Industry On Large Scale
PROJECT ACRONYM	TARGET-X
PROJECT WEBSITE	www.target-x.eu
PROJECT IDENTIFIER	https://doi.org/10.3030/101096614
PROGRAMME	HORIZON-JU-SNS-2022-STREAM-D-01-01 — SNS Large Scale Trials and Pilots (LST&Ps) with Verticals
PROJECT START	01-01-2023
DURATION	34 Months
DELIVERABLE TYPE	Deliverable
CONTRIBUTING WORK PACKAGES	WP6, WP2, WP4, WP1, WP3
DISSEMINATION LEVEL	Public
DUE DATE	M34
ACTUAL SUBMISSION DATE	M34
RESPONSIBLE ORGANIZATION	EDD
EDITOR(S)	Bart Mellaerts
VERSION	1.0
STATUS:	Final for upload
SHORT ABSTRACT	The deliverable represents the final report of work package 6. It collects and summarizes the learnings on technology enablers, documents the executed large-scale trial and summarizes findings from a questionnaire on 5G and future generations of mobile communications.
KEY WORDS	Energy, 5G, 6G, real-time, mmWave, positioning, AAS, RedCap, large-scale, learnings
CONTRIBUTOR(S)	Junaid Ansari (EDD) Jordi Biosca Caro (EDD)

	Maciej Muehleisen (EDD) Sascha Jaeger (EDD) Paul Becker (EDD) Pierre Kehl (IPT) Deniz Cokuslu (EBY) Lucas Manassés Pinheiro de Souza (RWTH-WZL) Mahdi Darroudi (NEU) Manuel Fuentes (FIVE) Niklas Beckmann (IPT) Janina Gauß (IPT)

Disclaimer

Co-funded by the European Union. Views and opinions expressed are, however, those of the author(s) only and do not necessarily reflect those of the European Union or the other granting authorities. Neither the European Union nor the granting authority can be held responsible for them.

Executive Summary

This deliverable (D6.5) constitutes the conclusive technical report synthesizing the results produced by Work Package 6 (WP6) within the TARGET-X project. WP6 was tasked with validating the applicability and performance of emerging mobile communication technologies — specifically 5G and exploratory 6G concepts — across a heterogeneous industrial ecosystem comprising multiple vertical domains. The deliverable articulates objectives, scope, methodological choices, and the principal outcomes of these validation activities.

The report describes the deployment of the project's identified "technology bricks" on one or more TARGET-X testbeds and explains how these components were integrated into the developed use cases. For each technology brick the document details the deployment strategy, configuration parameters, and the empirical evaluation procedures employed, including the performance indicators and measurement techniques used to assess metrics of interest for industrial communication.

In addition, the deliverable documents the experimental design, execution, and results of a large-scale trial conducted toward the end of TARGET-X, providing quantitative and qualitative evidence regarding system-level behavior and scalability in realistic industrial settings.

Finally, the report summarizes the findings of a cross-work-package questionnaire that solicited practitioner insights on deployment experience, operational challenges, and integration lessons. Drawing on these diverse sources of evidence, D6.5 offers an informed outlook on how insights from 5G deployments and early 6G research can guide future generations of mobile communications for industrial applications.

Table of Contents

List of Figures

List of Tables

List of Acronyms and Abbreviations

3GPP	3rd Generation Partnership Project: the standards body for cellular (GSM, UMTS, LTE, 5G/NR)
AOA	Angle Of Arrival
AIR	Antenna Integrated Radio
AMF	Access and Mobility Management Function: a 5G Core network function that handles registration, connection and mobility management

AMR	Autonomous Mobile Robot
BLE	Bluetooth Low Energy
BLER	Block Error Rate: fraction of data blocks/transport blocks received with errors
CCDF	Complementary Cumulative Distribution Function: statistical function showing $P(X > x)$
CDF	Cumulative Distribution Function: statistical function showing $P(X \leq x)$
DL	Downlink: radio direction from network (gNB/eNodeB) to UE
eMBB	Enhanced Mobile Broadband
FRER	Frame Replication and Elimination for Reliability: a mechanism (from TSN/industrial networking) to replicate frames on disjoint paths and eliminate duplicates for high reliability
FSTP	Financial Support for Third Parties
gNB	gNodeB: the 5G NR base station (RAN node)
GNSS	Global Navigation Satellite System: satellite positioning systems
KPI	Key Performance Indicator: measurable metric used to evaluate system performance
LIDAR	Light Detection And Ranging
LOS	Line of Sight: unobstructed direct path between transmitter and receiver
LTE	Long-Term Evolution: 4G mobile wireless standard
MEC	Mobile Edge Computing: hosting compute/storage at the network edge to reduce latency
MIMO	Multiple Input Multiple Output: antenna technology using multiple transmit/receive chains to increase capacity or reliability
MME	Mobility Management Entity: LTE core node responsible for mobility and session control
NFI	Near-Far Interference
NLOS	Non-Line-Of-Sight: radio path without a direct unobstructed line, typically via reflection/diffraction
NPN	Non-Public Network: a private cellular network (private 4G/5G deployment for an enterprise)
NR	New Radio: 5G radio access technology

NSA	Non-Standalone: 5G deployment option that uses 4G LTE control plane with 5G NR for user plane
OLOS	Obstructed Line of Sight: partial obstruction on the line-of-sight path causing attenuation
PDU	Protocol Data Unit: packet unit at a given protocol layer
QoS	Quality of Service
RAN	Radio Access Network: the radio part of the network
RSRP	Reference Signal Received Power: measured average power of reference signals
RSSI	Received Signal Strength Indicator
RTK	Real-Time Kinematic: GNSS technique for centimeter-level positioning
SA	Standalone: 5G deployment option using a full 5G Core
SSB	Synchronization Signal / Broadcast Block: 5G NR block that carries synchronization and broadcast information
TDD	Time Division Duplex: duplexing method where uplink and downlink share the same frequency but at different times
UE	User Equipment: the subscriber device
UL	Uplink: radio direction from UE to network
(UL)TDOA	(Uplink) Time Difference of Arrival
URLLC	Ultra-Reliable Low-Latency Communications: 5G service category targeting very high reliability and low latency for industrial use
UWB	Ultra-Wideband
WP	Work Package

1 Introduction

This deliverable reports the results produced by Work Package 6 (WP6) in TARGET-X, which investigated the role of 5G and prospective 6G technologies in enabling industrial use cases across multiple verticals (manufacturing, construction, automotive, energy, etc.). WP6's remit was to define, deploy and empirically validate modular “technology elements” (or technology bricks) intended to improve the performance, reliability and applicability of mobile communications in industrial scenarios. The present document consolidates those validation activities and situates them within the broader project context. The report explains how identified technology bricks were deployed on one or more TARGET-X testbeds and integrated into concrete use-case evaluations. For each assessed element the deliverable provides a rationale for its introduction, a description of the realization and deployment approach, and a summary of the empirical evaluation methods and outcomes. Where appropriate, certain technology assessments were carried out collaboratively with vertical work packages. These cross-work-package interactions are explicitly referenced throughout the report.

In addition to per-element evaluations, the document presents the design, execution and results of a large-scale trial conducted toward the end of TARGET-X. This trial was intended to produce a holistic, system-level appraisal of 5G for industrial communication and automation, including considerations of scalability, operational constraints and scenario diversity. The report details the trial setup, the rationale for selected test scenarios, measurement procedures, and the empirical findings arising from the execution phase.

The deliverable also includes a synthesis of qualitative insights gathered via a questionnaire distributed to all work package leads; responses contributed practitioner perspectives on deployment experience, integration challenges, and operational pitfalls. The ‘‘learnings and outlook’’ section integrates these practitioners inputs with empirical evidence collected during the two rounds of FSTP projects to derive implications for future generations of mobile communications in industrial contexts.

1.1 Objective of the document

The ambition of this report is to document the results of the empirical validation that was performed during the course of the project, documenting the introduced elements, how the empirical evaluation was performed, and which results were achieved. In some cases, the evaluation of a technology brick has also been performed in one of the “verticals” work packages.

1.2 Relation to other activities

WP6 has been interacting with most of the work packages during the execution of the TARGET-X project, and these interactions are reflected directly through references to validation activities performed and documented in the respective verticals WP. For the evaluation of RedCap, we executed a joint trial and split the documentation between our deliverables. WP4 executed the evaluations of the far-edge / edge continuum case, and with WP5 we evaluated mmWave propagation on a construction site.

The learnings and outlook section of this report was influenced by the joint work we did during the 2 rounds of FSTP projects.

1.3 Document overview

The deliverable is structured to present the different technology elements that were assessed in TARGET-X. Section 2 describes the details of the assessed technology brick, using a structure where first a motivation for the introduction is given, followed by a realization part and concluded by an evaluation part. Section 3 focuses on the documentation of the large-scale trial, by first describing the setup, followed by a motivation for the different test scenarios and concluded by documentation of the execution phase of the trial. Section 4 talks about the learnings that were collected during the project and provides an outlook view of the project towards future mobile communication generations. Section 5 concludes the report with findings and lessons learned.

2 Introduced technology bricks

2.1 Traffic differentiation and NW convergence

2.1.1 Motivation for introduction

The introduction of private 5G networks is a significant evolution in enterprise connectivity, offering dedicated, high-performance wireless infrastructure tailored to the enterprise requirements. In this regard, enterprise 5G networks are designed to support a diverse range of time critical applications. Each with unique network performance requirements, often based on throughput, latency and reliability [1]. To effectively manage such a wide range of applications and ensure optimal performance, the concept of traffic differentiation is key. Traffic differentiation involves classifying data traffic into distinct streams and applying specific actions to each stream. This approach ensures that different types of traffic receive appropriate treatment based on their requirements, especially when sharing network resources. An important goal is to ensure that critical data flows requiring uninterrupted service are prioritized over less time-sensitive traffic.

Such differentiated connectivity in 5G networks [2] is essential for unlocking the full potential of 5G and beyond systems.

2.1.2 Technical realization

The experimental setup to carry out traffic differentiation and network convergence is hosted at the factory environment of Fraunhofer IPT. The setup consists of an Ericsson commercial-off-the-shelf (COTS) 5G standalone (SA) private network, known as Ericsson Private 5G (EP5G). The EP5G [3] includes a cloud-based network management portal and troubleshooting app built to meet the requirements of enterprise IT and OT users. The 5G system features a QoS framework based on traffic priority segments. Five traffic segment levels are available for different enterprise services and priorities. Such traffic differentiation can ensure that time critical traffic is prioritized over best effort in scenarios with high loads.

In this regard, we develop an architecture solution to showcase the benefits of traffic differentiation in 5G enterprise deployments. The demonstration consists of the live streaming of a video feed from a USB camera and competing background traffic. An illustration of the architecture is shown in Figure 2-1. The host machine is connected to a USB camera, a screen display, a Cradlepoint 5G UE and a connection from the Core of the EP5G system. The USB camera streams a video feed over the air interface from a GStreamer [4](source) via the Cradlepoint 5G UE to the GStreamer (sink) connected to the EP5G Core. At the host machine, the received video feed is then displayed on a screen. To evaluate the performance of the traffic differentiation mechanism, an iperf3 client-server pair is used to generate background traffic.

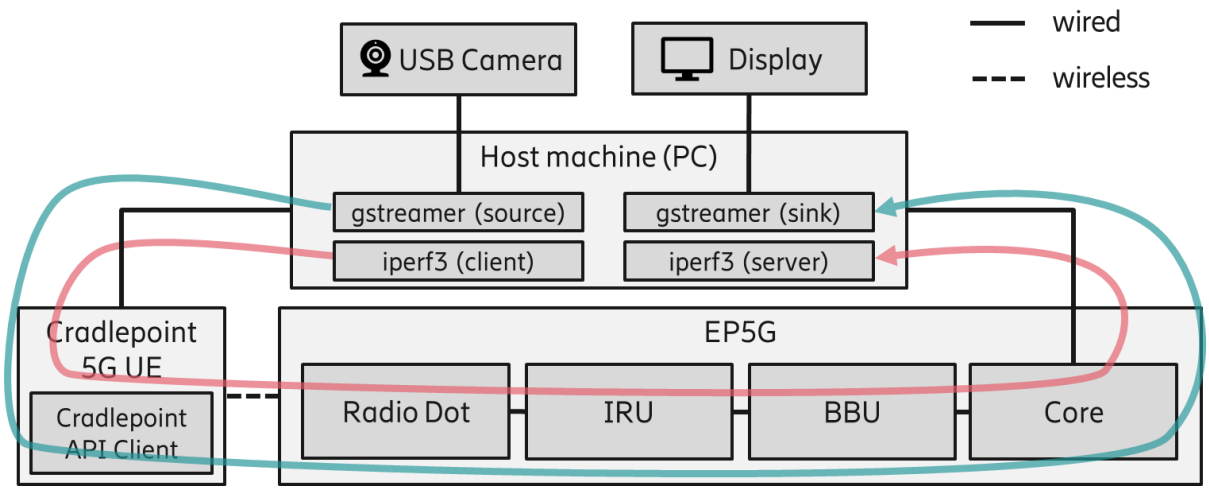

Figure 2-1: Architecture of the traffic differentiation setup

For traffic differentiation, EP5G allows to set a specific treatment based on the Data Network Names (DNNs). Two classes are defined for each of the DNNs, named as “Best Effort” and “Real-time Automation”. Internally, each DNN has a unique 5QI value from the range of non-standardized values (129 to 133). RAN configuration assures that the higher the 5QI value, the higher the priority. 5QI classes 129 to 131 are intended for streaming type of data, often using UDP. Radio Link Control (RLC) is therefore set to Unacknowledged Mode. Absolute Priority is used meaning e.g. that 5QI class 130 data is only sent after the 5QI 129 buffer was completely emptied. Classes 132 and 133 are intended for bulk data, typically using TCP. They are only transmitted when no 5QI 129 to 131 data is buffered for transmission. 5QI class 132 has Relative Priority (factor two) over class 133, as else there would be a high risk that 5QI class 133 does not get any opportunity to transmit (starvation), due to the greedy nature of TCP traffic. To showcase the capabilities of traffic differentiation in enterprise applications, we use a Cradlepoint R1900 router [5] which supports multi–Packet Data Network (multi-PDN), each PDN with own DNN [6], [7]. Such feature allows UEs to maintain multiple, simultaneous data connections to different networks services. This enables a single device to access the network services through different Packet Data Unit (PDU) sessions, with each session tailored to the specific requirements of the service. The router gets an IP address for each PDU session. The Cradlepoint 5G router provides an API to create filters steering different LAN traffic to different PDU sessions [8]. Such feature enables us to showcase the benefits of traffic differentiation using 5G systems for enterprise deployments as described in the following section.

2.1.3 Evaluation

To analyze the performance of the traffic differentiation mechanisms of 5G systems, we showcase the performance degradation of streaming a live video over 5G with and without differentiated connectivity.

Initially we stream the live video from the USB camera through the best effort segment (PDU session) of the industrial device. As can be observed in Figure 2-2(a), the quality of the video received from the GStreamer sink and displayed on the screen is good. Then the network is saturated with TCP traffic through iperf3, completely consuming the UL radio resources. The video stream and the background traffic are equally competing for the radio resources as they share priority (best effort). Therefore, the live streaming traffic is queued and longer delays occur, negatively impacting the

quality of the received feed as can be observed in Figure 2-2(b). However, when the live video is steered towards the high priority PDU session the image quality at the receiver is like the one observed without background traffic as shown in Figure 2-2(c). The quality of the video received is not degraded despite the network being highly loaded, showcasing the benefits of traffic differentiation in 5G systems.

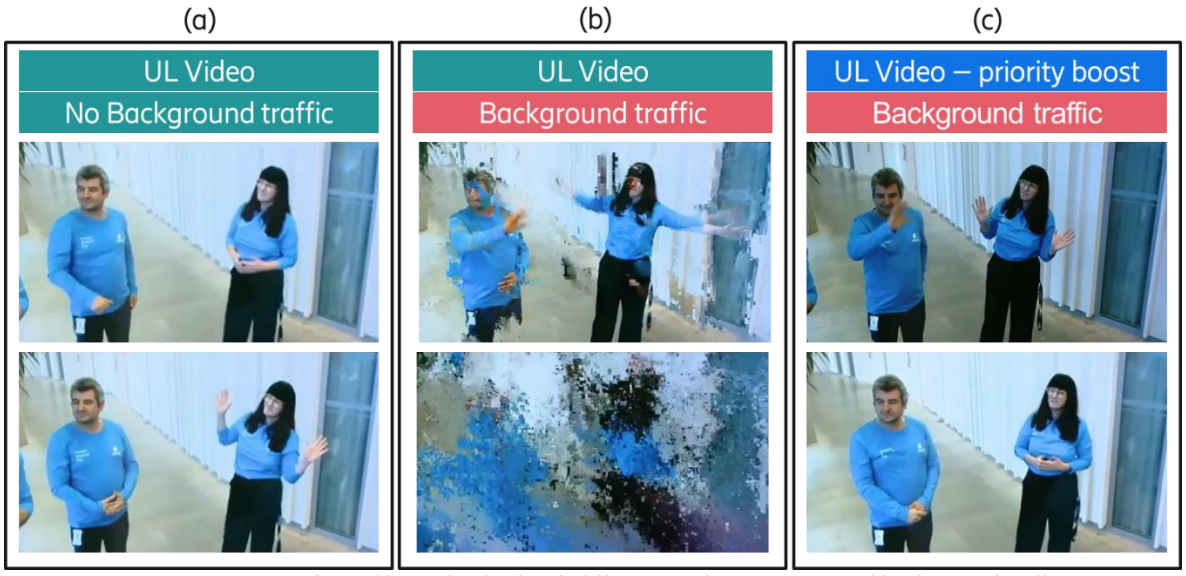

Figure 2-2. Screenshots of live video feed with differentiated connectivity and background traffic.

2.2 mmWave spectrum

2.2.1 Motivation for introduction

To address the growing demand for extremely high data rates, low latency and scalable connectivity, 5G New Radio (NR) supports key technologies and features such as massive multiple input and multiple output (MIMO), beamforming, carrier aggregation, flexible numerology and subcarrier spacing, wider channel bandwidths and introduction of new spectrum. The 3rd Generation Partnership Project (3GPP) Release 15 is the first set of standards enabling operation in both sub-7 GHz and millimeter wave (mmWave) dividing the spectrum into two frequency ranges (FR), FR1 (410 MHz to 7125 MHz) and FR2 (24.25 GHz to 52.6 GHz) respectively. Generally, FR1 is suitable for wide-area coverage owing to its good penetration through buildings and obstacles. On the other hand, FR2 supports extremely high data rates and low latency with its support for wider bandwidths and higher subcarrier spacing. For instance, FR2 supports single carrier bandwidths of up to 400 MHz and 240 kHz of subcarrier spacing. These capabilities are critical for applications like real-time robotics control, augmented reality and automated manufacturing among others. In Deliverable D5.1 [9] and Deliverable D2.3 [10] a number of use cases for mobile robotics in manufacturing and construction are described which require very high data rates with low latency. The mobile robotics use case in Deliverable D2.3 is centered around the integration of mobile manipulators within flexible assembly systems. The robot performs the task of pick-and-place of an industrial component. The industrial task involves key technologies such as machine vision for object detection, advanced motion planning algorithms for navigation and manipulation, simulation pipelines and real-time communication for outsourcing computational power. In this regard, a key element of the use case is to properly localize the robotics manipulator on the shopfloor for navigation and manipulation. A number of sensors may generate large data that require real-time processing in a central unit (normally edge computing servers). To ensure seamless edge-to-robot communication, the wireless network needs to support high throughput and low latency with high reliability. Hence, the use of 5G FR2 technology is essential to enable real-time communication.

2.2.2 Technical realization

2.2.2.1 Experimental setup

The performance evaluation of the 5G mmWave system has been carried out on the Fraunhofer IPT shopfloor in Aachen, Germany. The shopfloor covers approximately 2700 m^2, featuring over 50 machines of various sizes, and serves as a representative example of a realistic large-scale indoor industrial environment. As described in Deliverable 6.2 [11]2], the 5G deployment is based on a non-standalone (NSA) network. The anchor cell for mmWave devices is the LTE band 7 with 10 MHz of bandwidth. The anchor cell is only responsible for the signaling, initial attach procedure and connection establishment. The main traffic, including user data, is transferred exclusively via the related mmWave spectrum. In this regard, the 5G NR mmWave spectrum is licensed for private network deployments by the German spectrum regulatory authority, Bundesnetzagentur (BNetzA). The license provides 800 MHz of bandwidth allocation in the frequency range from 26.7 to 27.5 GHz. In the experimental setup, the licensed bandwidth is divided into eight component carriers (CCs) of 100 MHz each.

The mmWave 5G deployment setup at Fraunhofer IPT consists of two 5G NR radios in band B258. The radios are installed in different aisles of the shopfloor while being opposite each other as shown in Figure 2-3. Note that the 5G NR cells share the same LTE B7 anchor. The length and width of the shopfloor is 91 m and 27 m respectively.

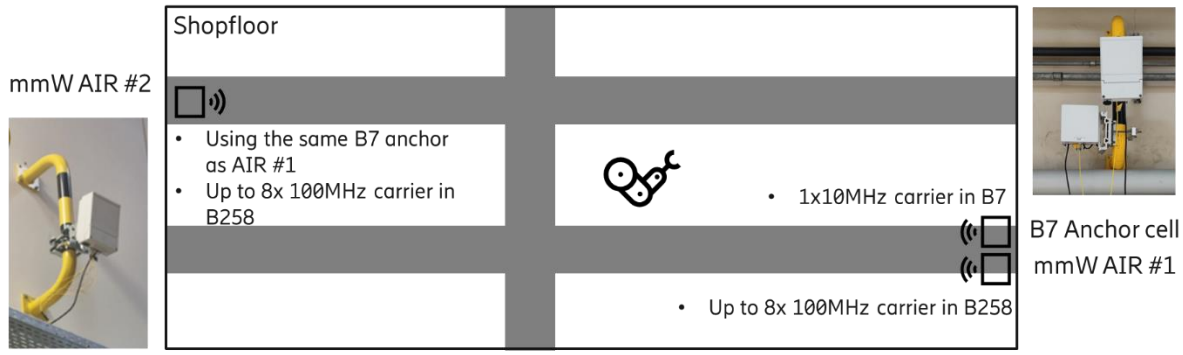

Figure 2-3: 5G NR NSA mmWave deployment architecture at Fraunhofer IPT.

In 5G systems enhanced beamforming capabilities are crucial for overcoming propagation losses and improving signal coverage and quality, particularly in FR2 deployments. Further technical details on the 5G network deployment at Fraunhofer IPT can be found in Table 2-1. In uplink (UL) transmission, we employ a prescheduling mechanism where the user equipment (UE) continuously receives transmission grants in advance without the need to explicitly request it. For our measurement campaign, we use commercially available end devices. As described in 2.2.2.2, the performance analysis of the results is based on the throughput, latency and reliability of the 5G system. Latency and reliability measurements are performed using a device with a Quectel RG530F-EU modem featuring a Qualcomm Snapdragon (SD) X65 platform. Throughput measurements are carried out using the Sony Xperia 1V, which is equipped with a Qualcomm SDX70.

Table 2-1: Technical details on the 5G network deployment at Fraunhofer IPT

5G SYSTEM	PARAMETER	DESCRIPTION/VALUE
5G NETWORK	Radio Unit	Ericsson AIR 1281
	Frequency band	258B
	Duplexing scheme	Time Division Duplexing (TDD)
	Frequency range	26.7 to 27.5 GHz
	TDD pattern	DDDSU, DDSUU, DSUUU
	TDD special slot pattern (D:G:U)	10:2:2 (DDDSU), 12:2:0 (DDSUU and DSUUU)
	Component Carriers (CCs)	8
	Bandwidth per CC	100 MHz
	Subcarrier Spacing	120 kHz
	Transmit power	2 W

5G END DEVICES	Device model	Quectel 5GDM01EK with Quectel RG530F-EU
	Chipset	Qualcomm SDX65
	FR2 MIMO capabilities	DL 2 x 2, UL 2 x 2
	Supported CCs	8 CCs DL, 4 CCs UL
	Device model	Sony Xperia 1V
	FR2 MIMO capabilities	Qualcomm SDX70
	Supported CCs	8 CCs DL, 4 CCs UL

As previously mentioned, the shopfloor at Fraunhofer IPT is divided into two aisles where machines are distributed on the sides and in the middle of the shopfloor. The middle area is further divided around the center of the shopfloor with a corridor that connects both aisles. For the experimental evaluation two deployment scenarios have been considered as shown in Figure 2-4. The analysis of the results is divided into a deployment scenario with one mmWave cell (Figure 2-4.a) and another with both mmWave cells (Figure 2-4.b). Such deployment scenarios allow us to investigate the performance of the 5G mmWave system under different line-of-sight (LOS) and non-LOS (NLOS) conditions. Due to the height of the antenna (ca. 5 meters) and the presence of machines, there is no direct LOS to the 5G radio on the opposite aisles. Furthermore, it allows us to evaluate the coexistence when multiple mmWave radios are deployed in a factory environment. Hence, we split the experimental scenarios based on the type of mmWave deployment.

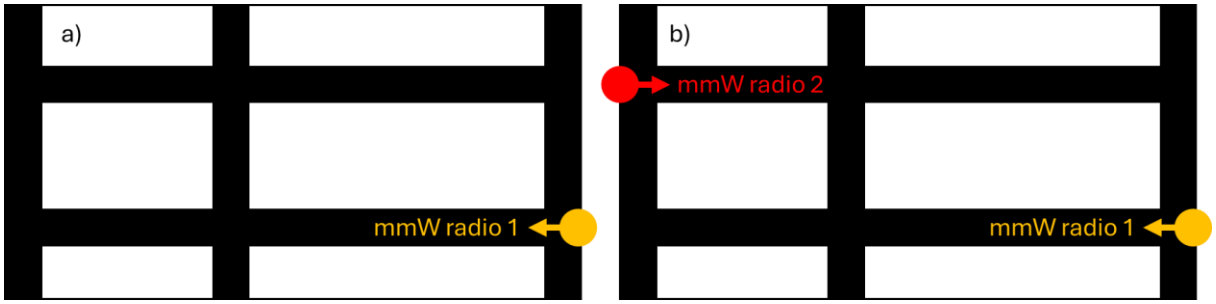

Figure 2-4. Deployment scenarios for the empirical evaluation of the 5G NR mmWave system at Fraunhofer IPT.

2.2.2.1.1 Single mmWave radio in an industrial environment

In this deployment scenario only one mmWave radio unit is enabled. This allows us to investigate the performance of the 5G mmWave system under different radio propagation conditions. While the placement of the radio unit is at the end of the aisle, it still ensures line-of-sight, even from the opposite end of the aisle, at a distance of approximately 90 m. Based on the deployment

characteristics of the robotics use case described in 2.2.1, three different UE locations have been identified from near-to-far relative to the radio for both LOS and NLOS radio conditions as shown in Figure 2-5. Shopfloor layout and various snapshots at Fraunhofer IPT with marked locations of the test device. . In our experiments, we further analyze the performance of the 5G mmWave system when the UE is placed inside a closed machine chamber (OLOS) [12] to realistically investigate the performance of the 5G mmWave system for a thermal camera use case [13]. During the experiments, we fix the orientation of the device. In LOS, the device antennas are aligned to the radio unit antennas. In NLOS locations, the device orientation is maintained such that the device antennas face the end of the hall where the radio unit is located, but they do not directly point to the radio unit itself. At OLOS, the device is facing the gas-filled double glass window of the laser robot machine chamber as shown in Figure 2-5.

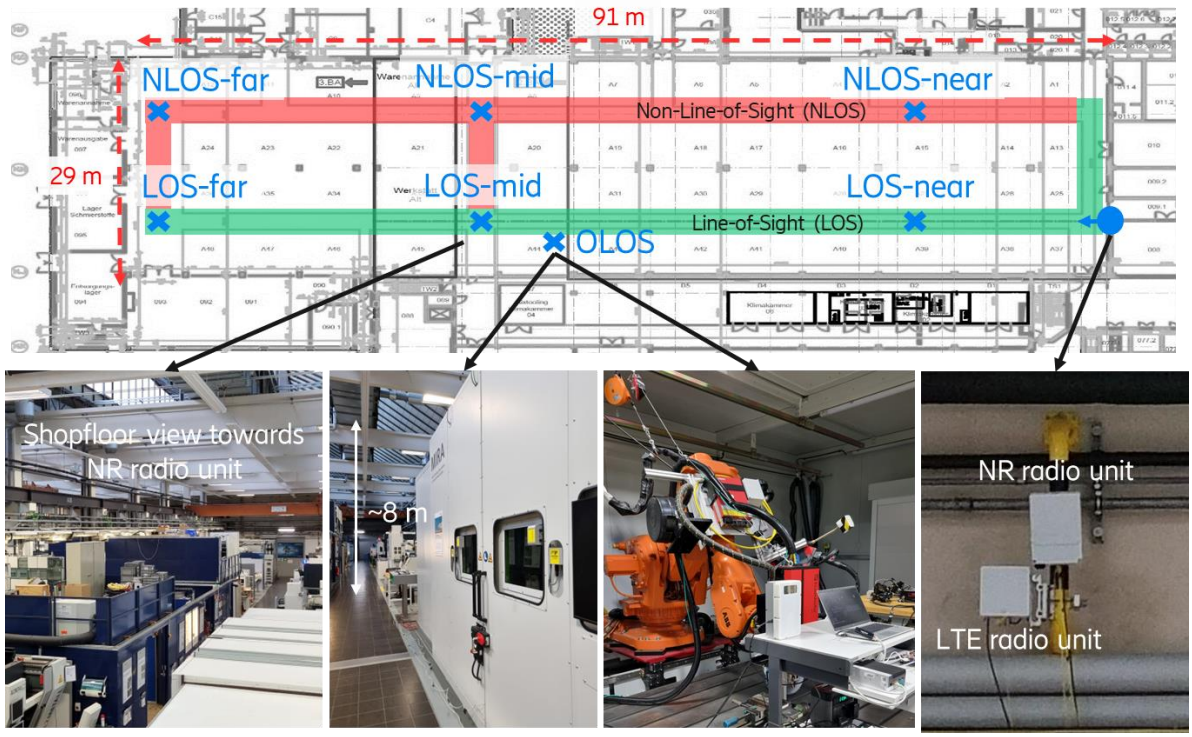

Figure 2-5. Shopfloor layout and various snapshots at Fraunhofer IPT with marked locations of the test device.

We explore another common use-case scenario in mobile robotics, e.g., when a robot navigates around on the shopfloor or when a workpiece moves between different automation cells in an assembly line. To mimic this scenario, we use a moveable trolley setup and move it between different test locations. In particular, we investigate the performance characteristics with a transition from a LOS to a NLOS position, and vice versa. We further explore the 5G system performance for different configuration parameters, such as TDD frame structure.

2.2.2.1.2 Multiple mmWave radios in an industrial environment

In this deployment scenario we aim to understand the performance of the 5G mmWave system when multiple radios are deployed in an industrial environment. Our focus is on the evaluation of the 5G mmWave system where two radios share spectrum resources. Thus, both mmWave cells can

leverage the 800 MHz of bandwidth available allowing for a more efficient use of the expensive radio resources. We compare network KPIs throughout the shopfloor compared to single cell deployment. We focus on how enhanced coverage improves network performance. Moreover, the increased complexity in deployment allows us to study potential interference effects. In particular, we investigate the co-existence under the co-channel interference [14]. As already mentioned, such deployment allows the factory owner to improve connectivity throughout the shopfloor and maximize the available bandwidth. In the context of the mobile robotics application, robots might be roaming around to perform their tasks. In such a scenario, the robots might be moving around from one mmWave cell to the other. When the two cells share spectrum resources inter cell interference might occur. From previous coexistence studies, it is noted that significant interference can be observed in the cell edge, e.g., on the transition area from one cell to the other. Therefore, we focus our empirical coexistence evaluation to the scenario shown in Figure 2-6. In this scenario, both test and interference devices are in NLOS radio conditions at the cell edge.

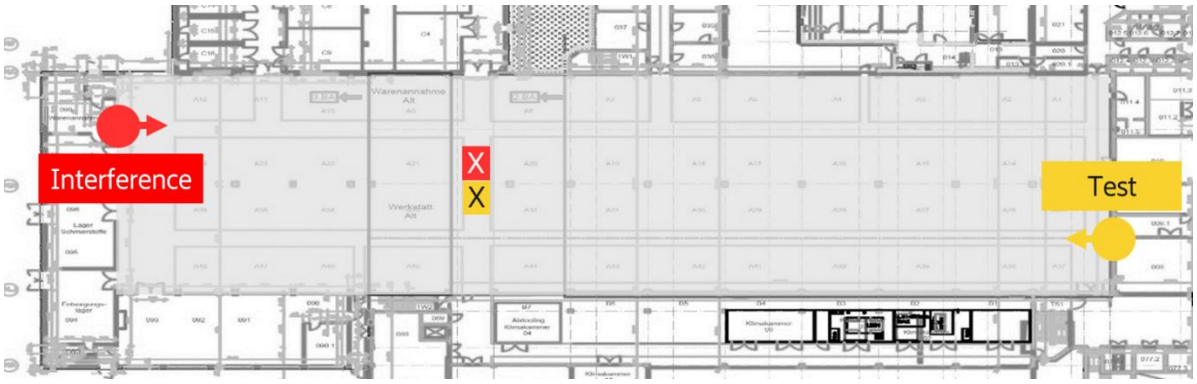

Figure 2-6. Coexistence deployment scenario where both test and interference UE are at the cell edge.

The antenna array of the test device is oriented towards the test gNB, while the interference device is placed next to the test device at a distance of ca. 20 centimeters. To evaluate the performance of the 5G system with and without interference we carry out two tests. Initially, the test device is receiving packets when the interference UE is powered off. Later, the interference device is powered on with DL heavy traffic generated to ensure that all the radio physical resources are occupied by the interference network. In this context, the test 5G system is under the so-called near-far interference (NFI).

2.2.2.2 Experimental methodology

We evaluate end-to-end one-way uplink and downlink communication performance of the 5G system with focus on three main KPIs: throughput, latency and reliability. The requirements of industrial applications often demand low latency, high reliability and high throughput to support data-intensive processes and maintain seamless connectivity for a large number of devices across the industrial shopfloor. We carry out one-way traffic for performance evaluation instead of two-way performance to understand the behavior of the industrial use cases relying on 5G connectivity. As described in [1], industrial use cases often exhibit asymmetric traffic profiles. Network configuration parameters can also influence the performance of the one-way traffic. For instance, FR2 deployments only support TDD deployments. Such deployments are particularly relevant for 5G non-public networks, especially indoors, as these allow tailoring resource allocation in uplink and downlink directions, according to the enterprise application requirements. In this deliverable, we

study three different TDD frame structures with different configurations of the downlink (D), uplink (U) and special (S) slots. One of the investigated TDD pattern allocates more resources to downlink transmissions (DDDSU), another balances the number of D and U slots (DDSUU) and the third pattern allocates more resources to uplink transmissions (DSUUU). D and U slots carry control information and data traffic for downlink and uplink, respectively. S slots consist of symbols mainly used for downlink transmissions (control and data) and some uplink transmissions (control), while also serving as guard (G) during the transition between the D and U slots.

To generate one-way traffic a field-programmable gate array (FPGA)-based tool is used. The FPGA-based tool allows us to emulate industrial traffic profiles and accurately measure one-way latency. The FPGA-based tool can be used to generate configurable automation traffic profiles. In order to avoid implementing a time synchronization setup between the sender and the receiver, the FPGA board is used as data sink for the 5G UE or the 5G network. Such a solution enables coherent timestamping with sub-millisecond clock accuracy. We evaluate the peak throughput performance using *iperf3*. In this context, the *iperf3* traffic is generated by an ASUS PC [15] which supports network interfaces with up to 10 Gbps. In both setups, the industrial traffic emulation and performance measurement device is connected to a 5G mmWave UE and the N6 interface of the 5G mmWave network as illustrated in Figure 2-7.

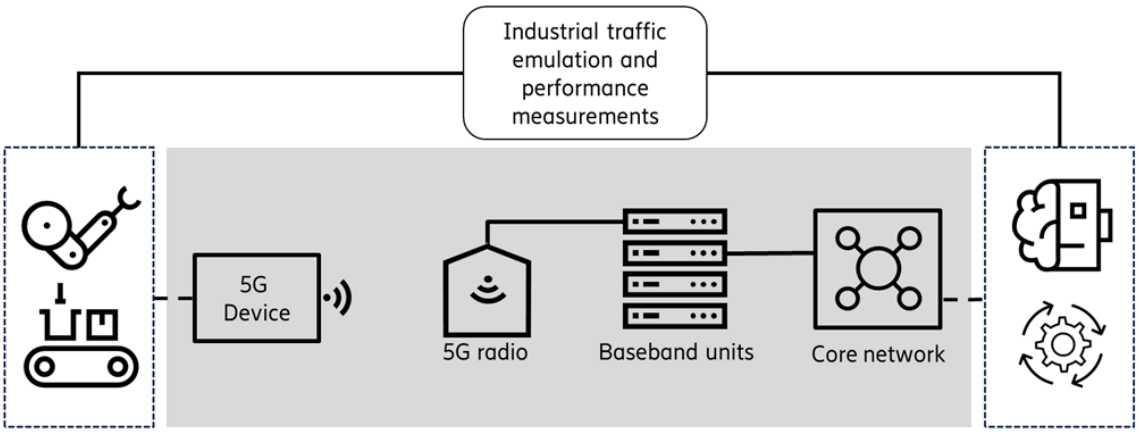

Figure 2-7. Schematics of the experimental setup used for emulating industrial traffic and carrying out performance measurements.

To analyze the latency performance, we collected at least 100,000 measurement samples for each experimental scenario to ensure our results are statistically significant. To evaluate the statistical significance of the data we calculate Student's *t*-distribution. We obtain the confidence intervals of multiple statistical values (e.g., mean, median, 90th percentile, etc.) of 5 equally sized batches from each time-series experiment. We collected at least 100000 measurement samples for each experimental scenario to ensure that our results are statistically significant. To evaluate the statistical significance of the data we calculate Student's t-distribution. We obtain the confidence intervals of multiple statistical values (e.g., mean, median, 90th percentile, etc.) of 5 equally sized batches from each time-series experiment. The overall empirical data collection and measurement campaign required several days of measurement time. Alongside the throughput and latency measurements, network tracing information is collected based on a tool developed to gather 5G network insights during the experiments. The tool allows access to network information from various nodes, including the Radio Access Network (RAN), Core Network and Transport Network. A

granularity of one second is used for gathering the aggregated network state and baseband tracing information to capture dynamic network behavior and monitor 5G mmWave performance behavior in an online fashion.

2.2.3 Evaluation

2.2.3.1 Performance evaluation of a single mmWave cell in a shopfloor

In this section, we evaluate the throughput, latency and reliability of the 5G mmWave system based on the experimental setup and methodology described in the previous section.

We preliminary assess the radio propagation conditions at different test locations on the shopfloor based on the single mmWave radio deployment. A static device is located at different locations, as illustrated in Figure 2-5. From the network traces, we observe that the synchronization signal block (SSB) reference signal received power (RSRP) decreases as (i) we move far away from the radio unit and (ii) undern NLOS conditions as shown in Table 2-2. The DL beam index indicates the spatial distribution of the beams for the different device's positions on the shopfloor.

Table 2-2. Radio propagation conditions and DL serving beam at different UE locations.

POSITION	SSB RSRP	DL BEAM INDEX
LOS-NEAR	-62.50 dBm	10
LOS-MID	-69.85 dBm	10
LOS-FAR	-74.50 dBm	10
NLOS-NEAR	-86.50 dBm	8
NLOS-MID	-92.63 dBm	11
NLOS-FAR	-98.10 dBm	8
OLOS	-100.32 dBm	10

We initially evaluated the capacity of the 5G mmWave system for three different TDD frame structures. For comparative analysis the device is facing the 5G radio with direct LOS at the middle of the shopfloor (LOS-mid in Figure 2-5) in all the experiments. The results in Table 2-3 clearly indicate higher DL throughput is achieved with a higher number of DL slots in the TDD pattern. Similarly, in UL an increasing throughput is observed for those TDD frame structures with higher allocation of UL slots. While the throughput in both UL and DL is generally high, it is important to

note that the overall UL throughput is constrained by the UE configuration support of a maximum of 4 CCs in UL. Unlike DL, where all 8 CCs can be utilized.

Table 2-3. Throughput in DL and UL for different TDD frame structures.

TDD FRAME STRUCTURE	DL THROUGHPUT	UL THROUGHPUT
DDDSU	3980 Mbps	923 Mbps
DDSUU	2940 Mbps	1390 Mbps
DSUUU	2150 Mbps	2120 Mbps

Furthermore, we carry out throughput measurements at NLOS test locations on the shopfloor to understand the effects of different radio channel conditions. In this context, one TDD frame structure (DDSUU) is selected for comparative analysis. As can be observed in Table 2-4, the change in radio propagation conditions clearly impacts the capacity of the system in NLOS. With almost 23 dB difference in the SSB-RSRP values, the 5G system selects lower modulation and coding scheme in the NLOS position to compensate for the challenging radio conditions compared to LOS.

Table 2-4. Throughput comparison in LOS and nLOS conditions for the TDD frame structure DDSUU.

POSITION	DL THROUGHPUT	UL THROUGHPUT
LOS-MID	2940 Mbps	1390 Mbps
NLOS-MID	1140 Mbps	91 Mbps

Latency and reliability aspects of the 5G system are also evaluated. The DL and UL latency results for a deployment scenario with direct LOS, at the middle of the shopfloor with DDSUU TDD frame structure are shown in Figure 2-8. At this location the radio propagation conditions are favorable as the static device has direct LOS to the NR radio unit. The results indicate a mean performance of 1.46 and 2.22 ms for DL and UL respectively.

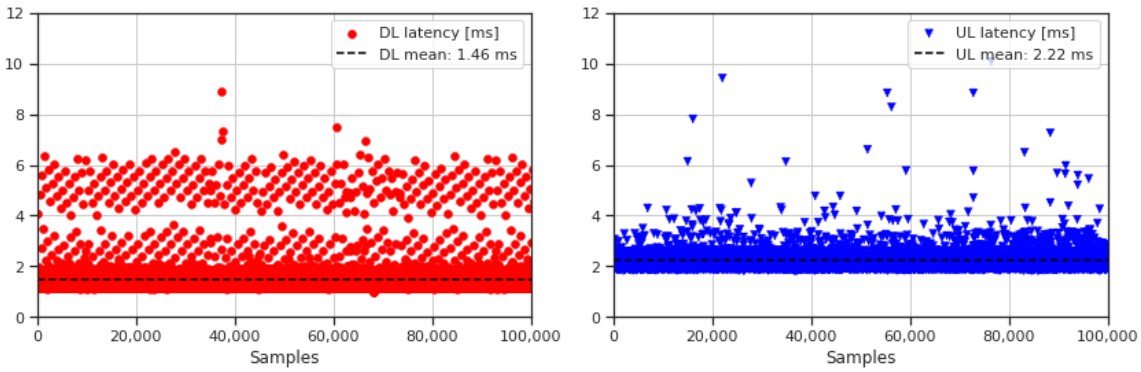

Figure 2-8. DL (left) and UL (right) latency time series [ms] at LOS-mid with TDD pattern DDSUU.

Nevertheless, the time-series results lack a statistical significance of the 5G system for industrial use cases with low latency and high reliable requirements. In this context, reliability is defined as the percentage value of packets successfully delivered within the delay constraint. For example, in a mobile robotics application, 10 ms of communication latency (one-way) with successful packet delivery is to be guaranteed 99.9% of the time [16]. Therefore, we present the complementary cumulative distribution function (CCDF) to evaluate the latency results as shown in Figure 2-9 (left). The CCDF is presented in a logarithmic scale to indicate the latency reliability with its bounded delays for high percentiles. The results indicate that the peaks observed in the time-series represent less than 1% of the sample set. Nevertheless, the differences between the UL and DL distribution are explained by the moderately large number of retransmissions in DL and the different scheduling mechanisms. Furthermore, in our experimental setup, the maximum configured modulation is 256 QAM and 64 QAM for DL and UL, respectively. Additionally, we evaluate the confidence intervals of the sample set based on Student's *t*-distribution for different percentiles in Figure 2-9 (right). The sample set of each experiment is equally divided into five smaller sample sets. The confidence intervals are obtained based on statistical percentiles (50th, 90th, 99th and 99.9th percentile) of the small sample sets under evaluation for each of the experiments. The highest percentage difference in the confidence intervals 4.3% in the 99.9th percentile in DL. The results obtained determine that our sample set of 100000 samples is sufficient to reliably estimate the values up to the 99.9th percentile.

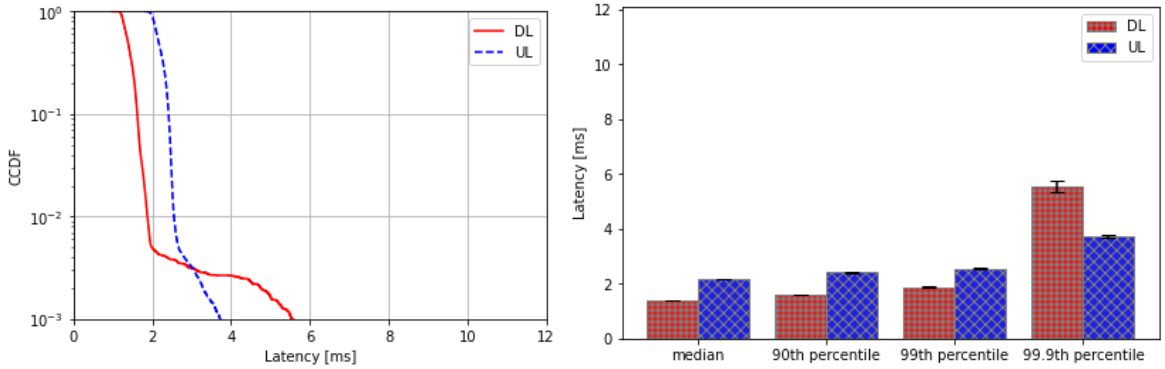

Figure 2-9. UL and DL latency CCDF (left) and bar graphs (right) of selected percentiles with confidence intervals.

We further evaluate the latency and reliability of the 5G system when the test device is located at different locations on the shopfloor as illustrated in Figure 2-5. The analysis is based on the results for the TDD pattern, DDSUU. The results in Figure 2-10 (left) indicate that, for the most challenging radio conditions (NLOS-far and OLOS), the 5G system is capable of ensuring low-UL-latency bounds with high reliability (below 4 ms at 99.9th percentile). In DL, the latency under NLOS conditions, when the device is near the base station, remains comparable to scenarios where the device antennas maintain LOS with the 5G mmWave base station antenna as shown in Figure 2-10 (right). However, as the device moves to a faraway scenario, the median values increase in NLOS conditions. This increased delay is caused by the challenging radio conditions. Similar latency can be observed when the device is placed in a machine chamber under OLOS conditions. At this location, the device is closed in a machine chamber with some windows (as shown in Figure 2-5) causing similar effects as when the device is far away in NLOS conditions. The DL results indicate that the device suffers in challenging radio conditions. While advanced, the device antenna receivers suffer in mitigating the effects of multipath propagation in mmWave deployments.

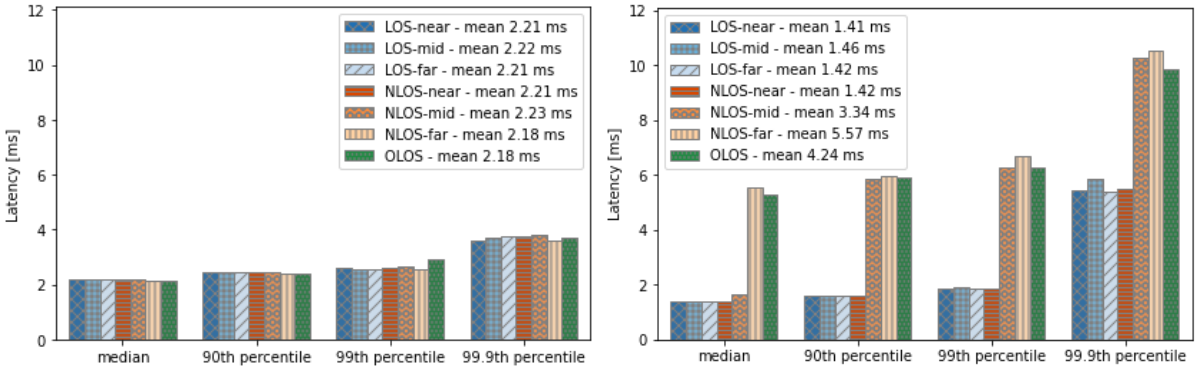

Figure 2-10. UL (left) and DL (right) latency of the 5G mmWave system for different locations with LOS, NLOS and OLOS scenarios.

Finally, we investigate the performance of the 5G mmWave system when a UE is moving between positions with LOS and NLOS coverage for the single radio deployment scenario. In Figure 2-11 we analyze the performance of a moving device from positions in the middle of the shopfloor from LOS to NLOS and vice versa. Due to the changing channel conditions, the 5G mmWave system accordingly applies to a more robust or optimistic MCS selection. As a more optimistic (higher value) MCS in LOS conditions tend to carry larger data portions over the air, the transport block must be divided in smaller data transmissions for some NLOS scenarios due to more robust (lower value) MCS selection.

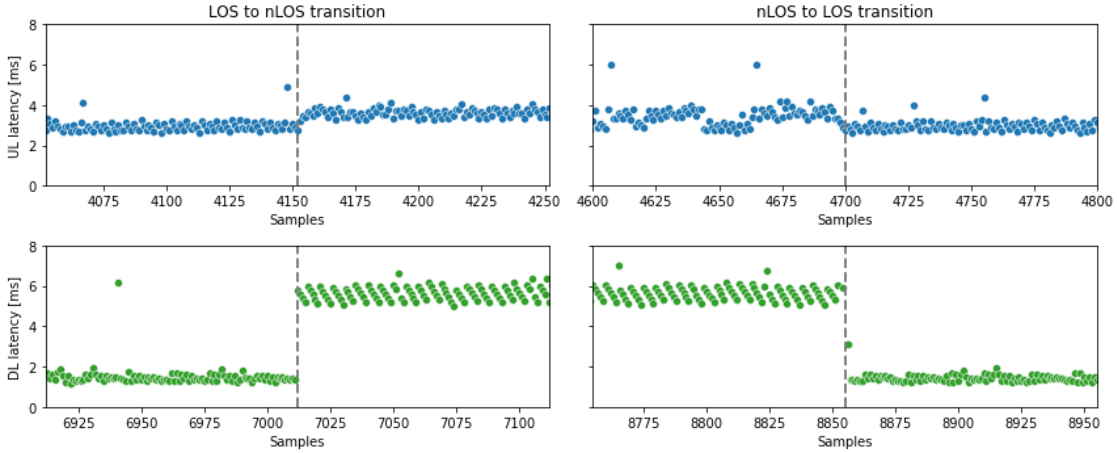

Figure 2-11. Zoomed-in portion of the UL and DL latency for static and moving UEs showing transitions from LOS to NLOS (left) and NLOS to LOS (right) scenarios.

Further details of the empirical performance evaluation of the 5G mmWave system can be found in [13].

2.2.3.2 Performance evaluation of multiple mmWave cells in a shopfloor

We evaluated the performance of a 5G system using multiple mmWave cells in a factory environment. Our goal is to mainly understand how DL throughput, latency and reliability are affected at the edge of the network coverage, where signals from the two mmWave radios overlap and interfere with each other. Following up on the previous studies on the 5G co-channel

coexistence, which showed that DL performance suffers when devices are nearby, we set up a specific test scenario. As shown in the schematic in Figure 2-5, we place two devices in a corridor of the Fraunhofer IPT shopfloor. Each device is connected to a different 5G radio with non-line of sight (nLOS).

The results, illustrated in Figure 2-12, show how the system performs with and without interference from the neighboring cell. The red results indicate the performance without interference, where the interference network is disabled. The blue results indicate the DL performance when there is DL NFI. In this case, the interference system is generating high load traffic in DL. The DL latency and reliability results indicate that no significant interference issues are observed. During the latency experiments the radio channel conditions (RSRP) were consistently good at approximately -77 dBm. However, the DL throughput drops ca. 18% (60 Mbps[1]) with DL NFI compared to the no interference case. Further insights from the baseband traces indicate very similar RSRP although with a slight difference on the reported Channel Quality Indicator (CQI) values. Dropping from 12.62 to 10.96, respectively. This small change triggers the link adaptation algorithm to select more robust, but less efficient MCS. Using a lower MCS reduces the number of bits transmitted over-the-air resulting in the lower average DL throughput. Particularly, the difference in MCS selection is driven by the inner loop link adaptation as the difference on the number of retransmissions is marginal.

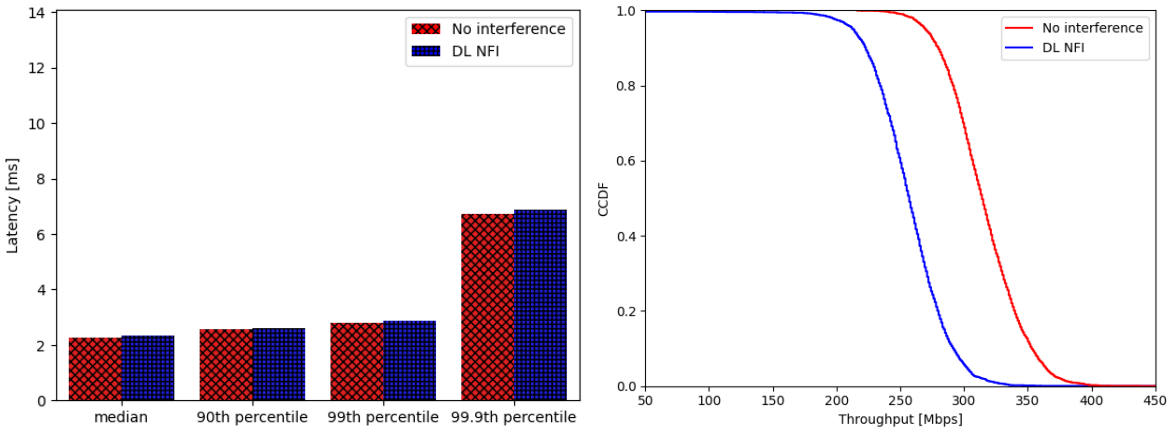

Figure 2-12: Performance with and without interference from the neighboring cell

Despite the throughput reduction, our results indicate the overall robustness of the 5G mmWave system in a factory environment with coexisting cells. The system maintained highly reliable performance for both latency and throughput with almost no data retransmissions required. This highlights the beamforming capabilities of 5G mmWave systems and the robustness despite non line of sight radio conditions.

[1] The throughput difference is attributed to the use of a single component carrier (CC) with 100 MHz bandwidth.

2.3 5G positioning

2.3.1 5G NR indoor positioning

2.3.1.1 Motivation for introduction

Indoor positioning cannot rely on satellite-based GPS, as it is the case for outdoor. There are already several technologies on the market for precise indoor localization, for example UWB (Ultra-Wideband, BLE (Bluetooth Low Energy), Indoor GPS, Laser tracker. In addition, there are LIDAR or camera-based systems, which could also be used for Simultaneous Localization and Mapping. They all require specific targets on the object and high investments in a dedicated infrastructure. 5G based localization does not require any additional HW and is in Ericsson's current implementation device-agnostic. It makes use of the existing indoor radio network deployment.

An accuracy of 1-3m already allows for realization of use-cases like asset tracking or global localization as described in Figure 2-13.

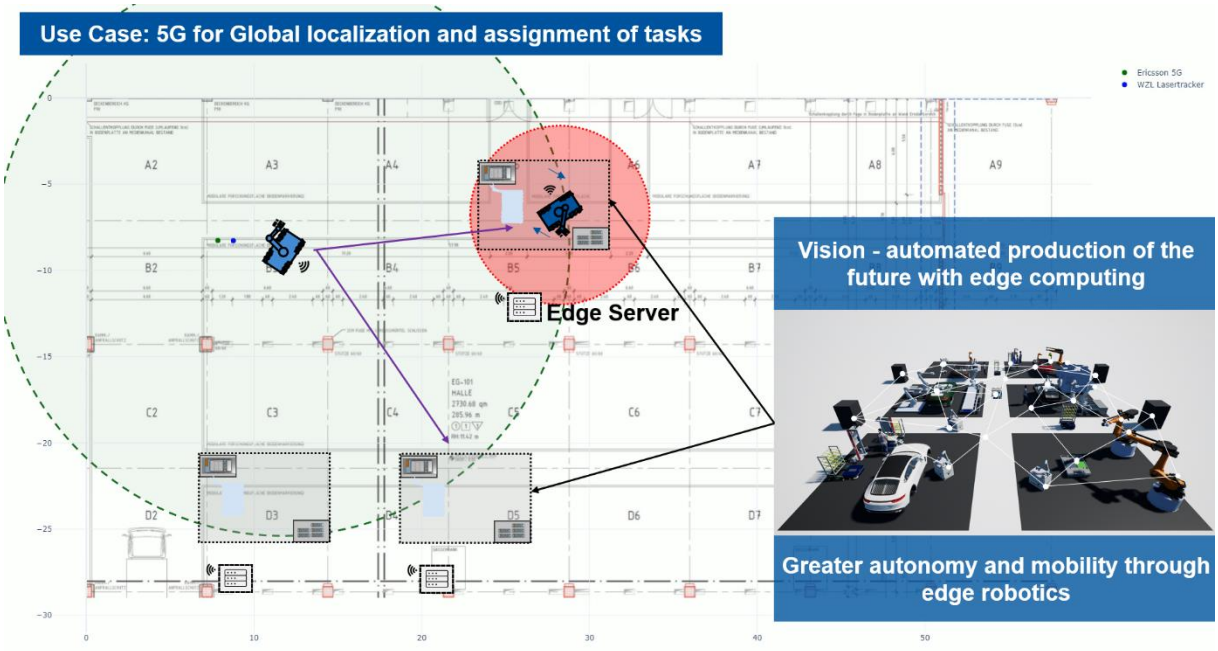

Figure 2-13: Visualization of 5G for global localization and assignment of tasks

2.3.1.2 Technical realization

As an extension to the existing non-standalone (NSA) 5G indoor network an advanced positioning PoC system was deployed in the Laboratory for Machine Tools and Production Engineering (WZL), which belongs to RWTH Aachen University and is part of the Industry Campus Europe (ICE). The NSA system operates on 3.7 – 3.8 Ghz with a bandwidth of 100 Mhz. Figure 2-14 shows the system architecture. 7 Radio Dots or Transmission Reception Points (TRPs) are used to cover a large part of the factory hall.

Radio Interface Based Monitoring (RIBM) is used to synchronize and correct timing between the TRPs. This is a prerequisite for decent accuracy using time measurements for the position estimates. In our prototype setup a steady data call was established by means of the iperf3 tool to receive a

recurring DeModulation Reference Signal (DMRS) from the UE on which the Uplink Time Difference of Arrival (UTDOA) measurements are executed.

A Positioning Function and Control PC (PFC) receives the UTDoA and RIBM measurements and uses MATLAB with hyperbolic trilateration algorithms to locate the UE position.

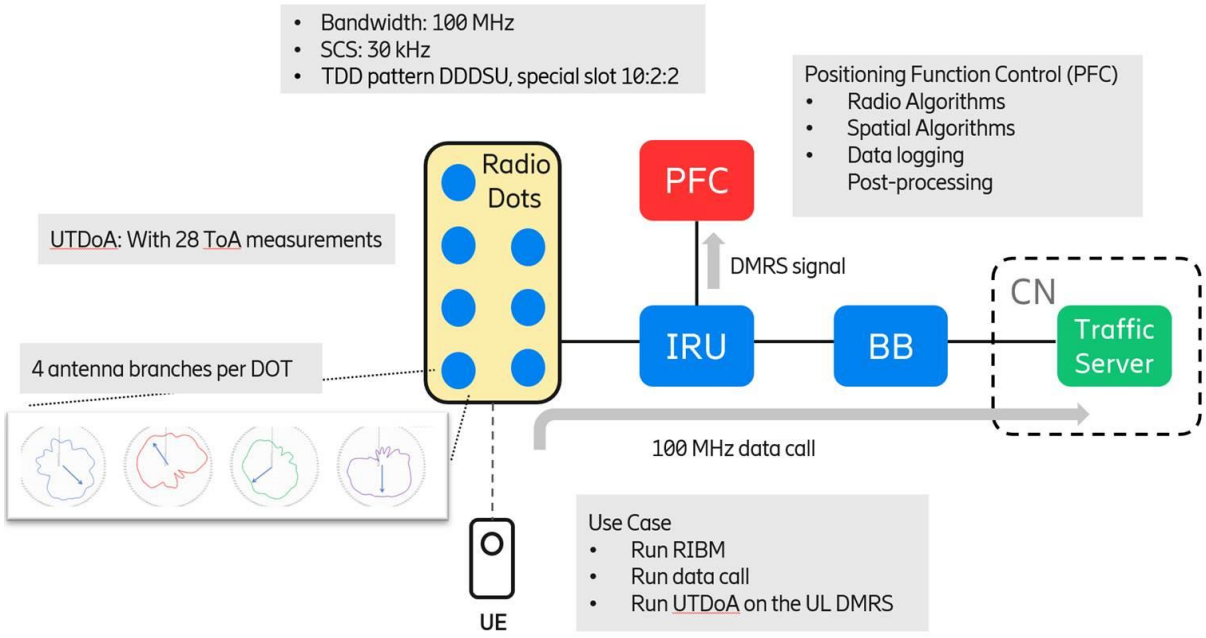

Figure 2-14: 5G Indoor Position PoC architecture

Figure 2-15 gives an overview of the entire setup at WZL, including location of the TRPs/Radio Dots and static test points. Measurements have been repeated several times on different days.

Dynamic measurements were done with an autonomous mobile robot (AMR) Kairos UR10 from Robotnik, where the mobile device was mounted either on the platform at 50 cm or on the robot arm at approximately 1,10m and later at 1,50m.

For static measurements, the mobile device was mounted at 1,50m on a tripod or the robot arm.

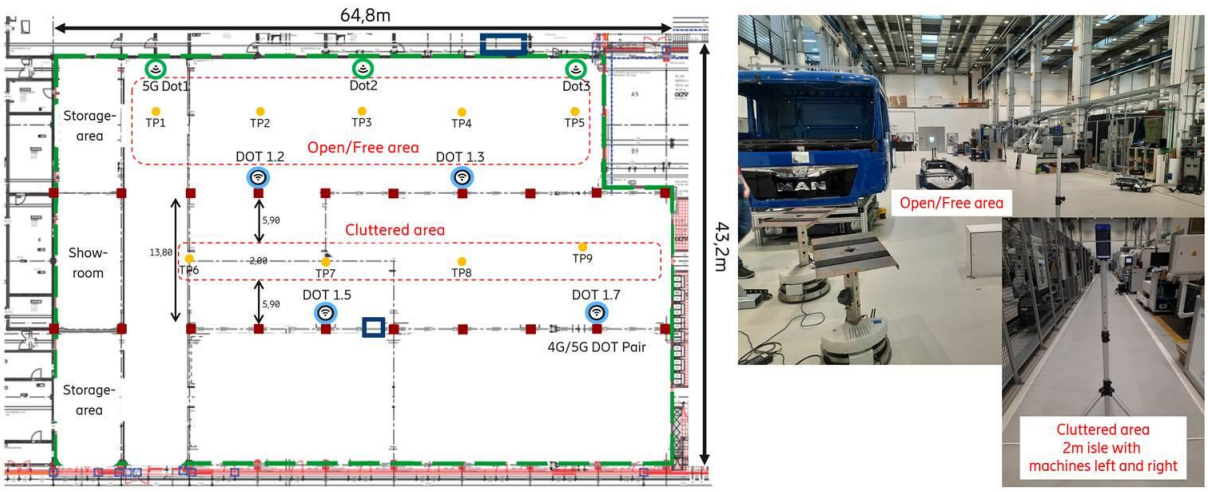

Figure 2-15: Shopfloor overview with static test points

Initially postprocessing was done on collected data sets over 300 samples, allowing to process the same data with different algorithms. Static measurement points were determined by a laser range finder. Dynamic measurements started with simple movements along a straight line, determining start and end point also with a laser range finder.

The MATLAB scripts deliver floor plan showing ground truth vs. 5G position estimates and CDF plots for accuracy. Ground truth means the exact reference position, determined by most accurate tools like laser range finder, as mentioned above.

An example is shown in Figure 2-16 below.

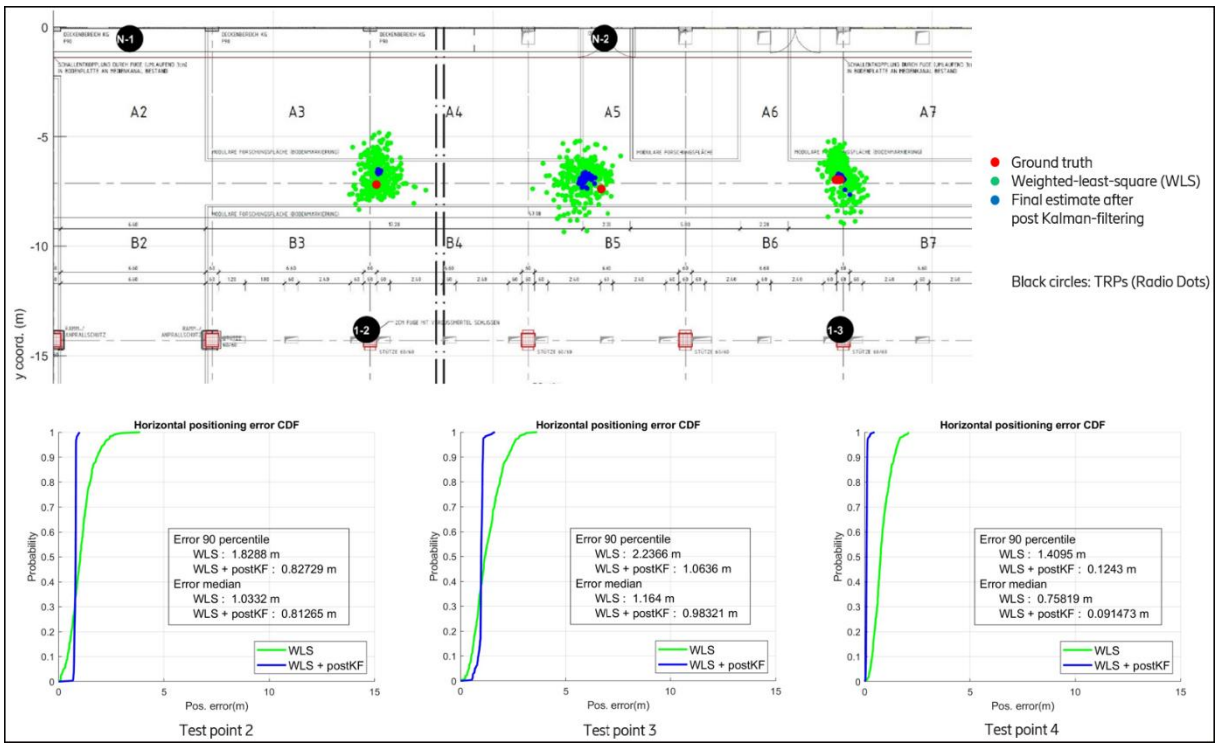

Figure 2-16: Static measurement results with shopfloor map and Cumulative Distribution Function for positioning error

At a later stage, the 5G system has been integrated with the existing metrology system at the Line-less mobile assembly laboratory at WZL, allowing us to see 5G positioning estimates in real-time and benchmark against more accurate systems like laser-tracker or camera-based motion tracking system. The high-level architecture is depicted in Figure 2-17.

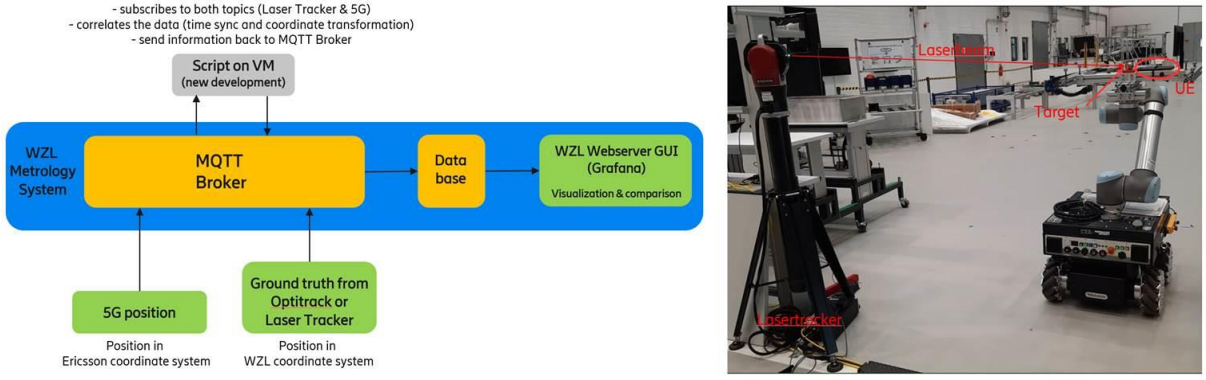

Figure 2-17: Architecture overview

Figure 2-18 below shows an example for the output delivered by the MATLAB scripts on the PFC. Here a laser-tracker was used as ground truth reference.

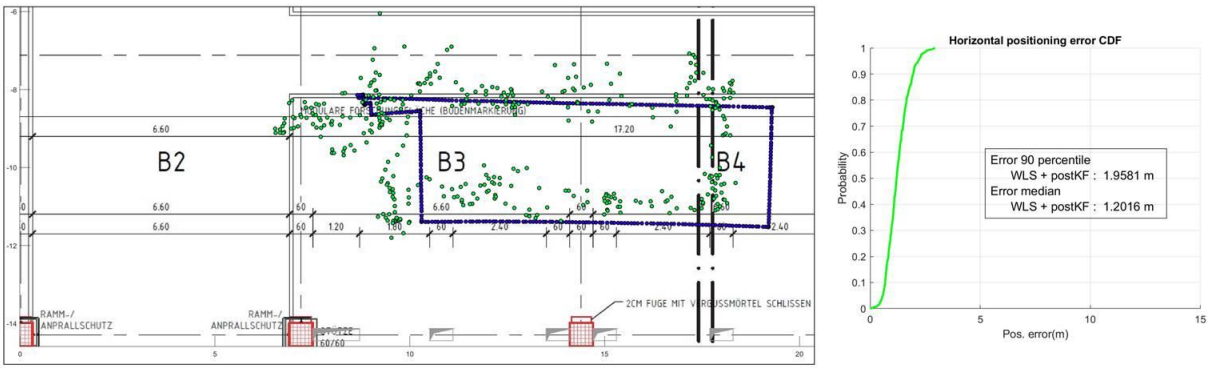

Figure 2-18: Measurement results from moving AMR

Towards the end of the project the camera-based OptiTrack system could be used as ground truth reference and several measurements have been made in this setup.

2.3.1.3 OptiTrack System as Ground Truth

An OptiTrack system [17] is a motion capture (MoCap) solution widely employed in robotics, virtual reality, biomechanics, and animation to deliver precise position and orientation tracking of objects or individuals. The system operates through an array of infrared cameras positioned around a designated tracking area, which detect retroreflective markers affixed to the tracked objects. These data are processed by a central unit that triangulates the marker positions and computes the full six degrees of freedom (6-DoF) pose—encompassing both position and orientation—of rigid bodies in real time. With properly calibrated setups and sufficient camera coverage, OptiTrack systems can track volumes ranging from a few to several tens of square meters, achieving sub-millimeter accuracy. Due to this high precision, low latency (typically a few milliseconds), and independence from onboard robot sensors, OptiTrack is commonly used as a ground truth reference in robotics research, particularly for benchmarking localization and control systems that rely on accurate 6-DoF state estimation. Installed in the WZL testbed is an OptiTrack System. It consists of 38 Units of PrimeX 41 infrared cameras from NaturalPoint Inc.[18], mounted on the ceiling to provide full coverage of the workspace, as illustrated in Figure 2-19. The system is designed for high-precision motion tracking and, when fully calibrated and configured using Motive, the official software provided by OptiTrack, can achieve a positional accuracy ranging between 0.2 mm and 0.5 mm.

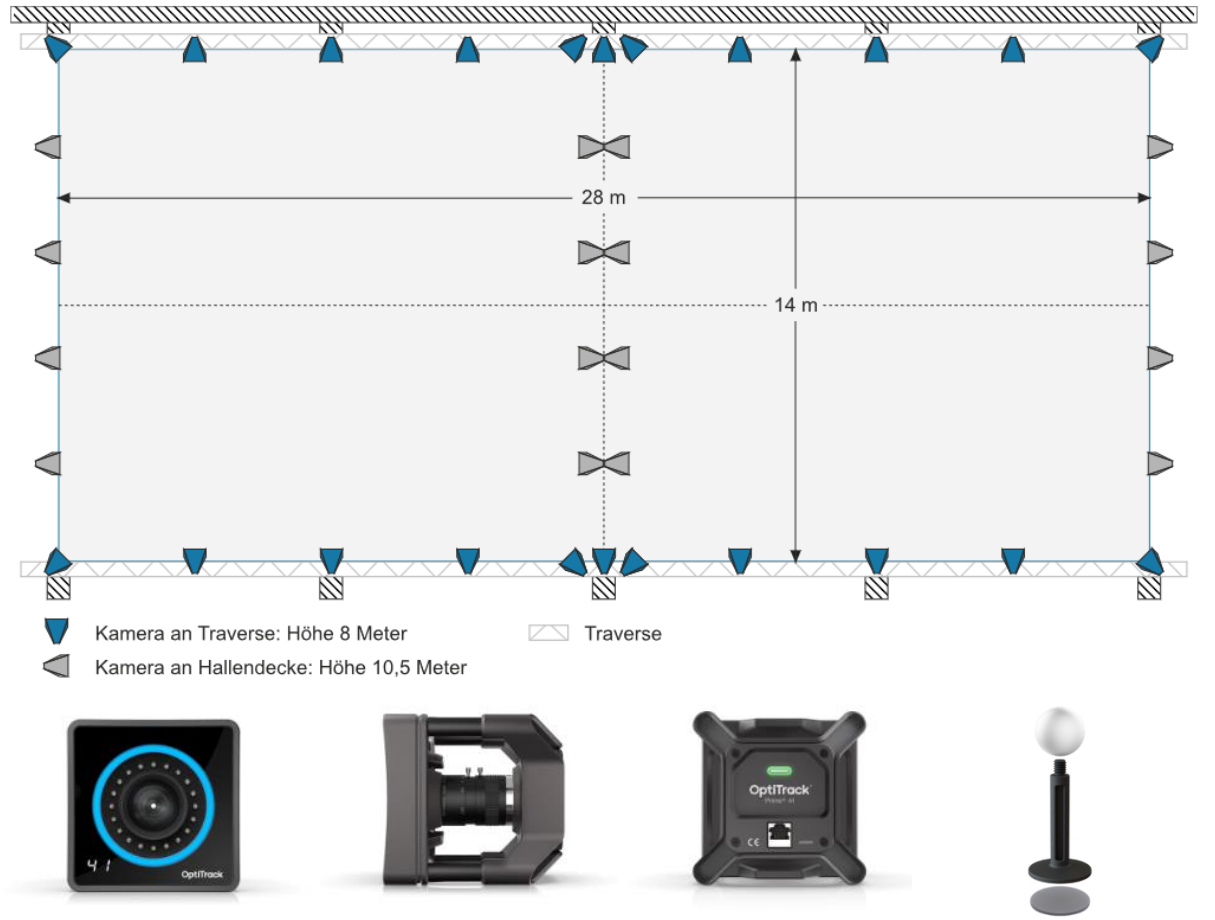

Figure 2-19: OptiTrack system deployment at RWTH WZL

During our experiment, 26 of the 38 infrared cameras were actively used with a reduced accuracy of approximately 3 to 4 mm. Despite this lower precision, the setup was sufficient for tracking rigid body markers attached to the robot involved in the experiment, as illustrated in Figure 2-20. The operating environment of the robot, used for the positioning trial is shown in Figure 2-21 (a). The system operated at a capture rate of 240Hz, which allowed real-time position data to be streamed and recorded, as shown in Figure 2-21 (b).

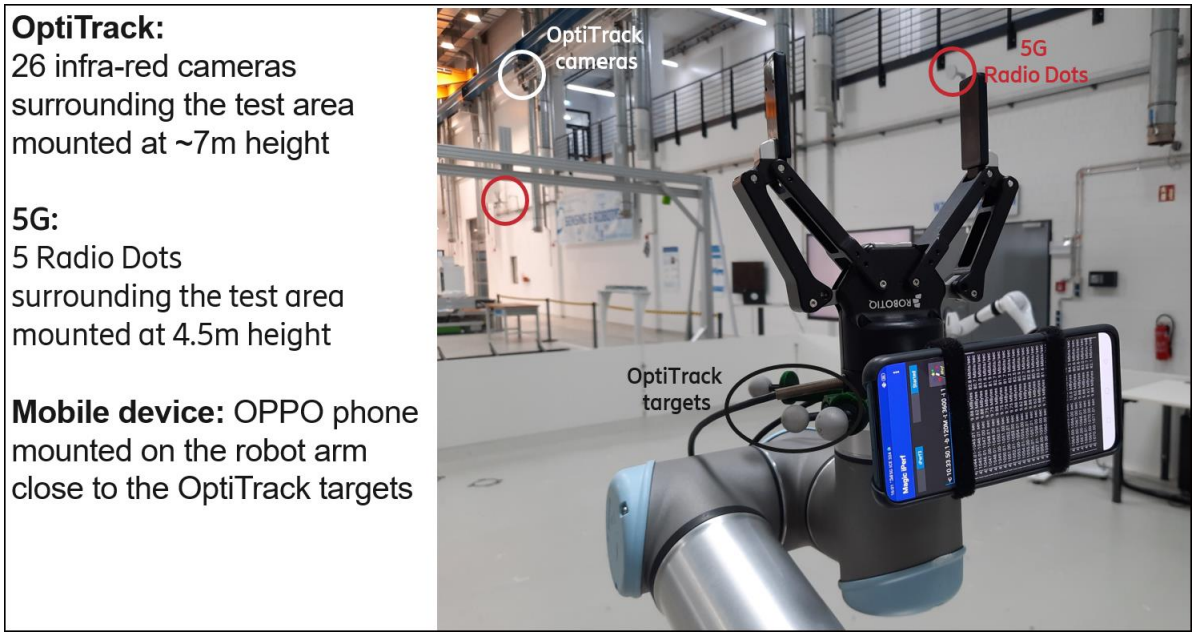

Figure 2-20: OptiTrack and 5G positioning combined setup

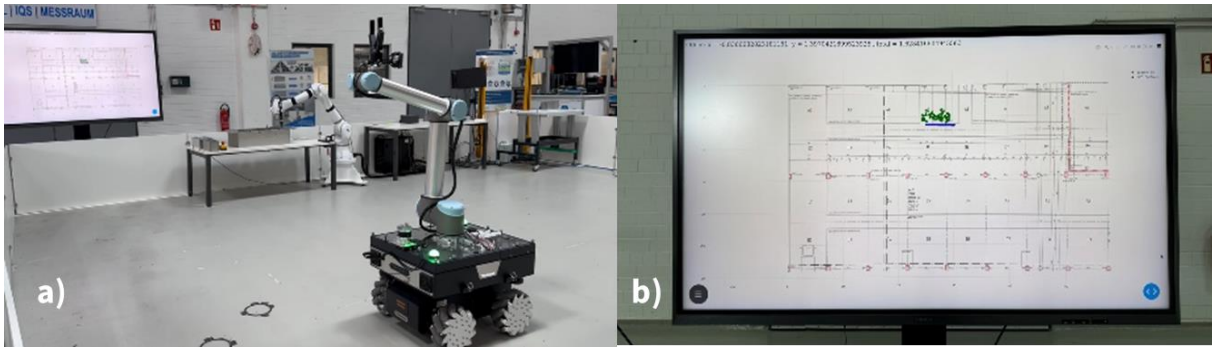

Figure 2-21: Positioning execution environment (a) and detail of real-time positioning plotting (b)

2.3.1.4 Evaluation

In the context of positioning, accuracy refers to how close a measurement is to the true or actual location, while precision refers to the consistency or repeatability of measurements.

Precision of the used 5G system has been evaluated by taking 300 measurements of the same static position.

E.g. in Figure 2-16 Test Point 2 is showing high precision and an almost constant distance of ca. 80cm to the true location. Samples for Test Point 3 are a bit more scattered at an average distance

of 1m from the true location, i.e. less good precision. Test Point 4 shows high precision and high accuracy with a few outliers.

Results from static measurements are summarized in Table 2-5 below.

Table 2-5: Static measurements: Accuracy for 90% of all samples

TEST POINT	GROUND TRUTH REFERENCE	
	Laser tracker	OptiTrack
TEST POINT 1	0.45	*)
TEST POINT 2	0.75	*)
TEST POINT 3	1.04	*)
TEST POINT 4	0.20	2.07
TEST POINT 5	1.61	1.39
AVERAGE	0.81	1.73

*) Test Points could not be measured anymore, because this area of the shopfloor got occupied

Measurements have been repeated on several dates with laser tracker and OptiTrack as ground truth reference. Accuracy and precision vary depending on location and are significantly impacted by obstacles and reflective surfaces, causing NLOS signals or reducing number of LOS signals.

The extreme difference for TP4 might be caused by significant increase of metal pieces on the whole shopfloor.

During dynamic measurements the AMR was moving at a speed of approximately 0.25 m/s along a straight line or a square. Here each ground truth position was matched with one estimate from the 5G system. Therefore, precision could not really be determined. Accuracy was in general worse than for static measurements, see Table 2-6 and Table 2-7 below. The values represent the average from repetitive measurements.

Table 2-6: Straight Line measurements: Accuracy for 90% of all samples

SPEED	GROUND TRUTH REFERENCE	
	Laser tracker (15m line)	OptiTrack (6m line)
SPEED 0.25M/S	2.27m	2.20m
SPEED 0.50M/S	3.44m	not done

Table 2-7: Square shape measurements: Accuracy for 90% of all samples

SPEED	GROUND TRUTH REFERENCE	
	Laser tracker (8.50m x 3m)	OptiTrack (6m x 2m)
SPEED 0.25 M/S	1.96m	2.27m

Conclusion:

With the current accuracy of 1-3m, 5G positioning already allows for realization of use-cases like asset tracking or global localization as described before. For automated production accuracy in the range of millimeters and 6D pose estimation would be required.

A commonly used technique for this is SLAM based on camera or LIDAR images or a combination of both. Camera-based SLAM, on the other hand, relies on visual features in the environment. It's more sensitive to lighting, motion blur, and texture availability — but has advantages in cost and availability, since standard cameras are cheaper and lighter. Visual SLAM can also capture rich color and texture information, which LIDAR cannot on its own, making it better for visually rich 3D reconstructions.

In practice, LIDAR maps tend to be more geometrically accurate and robust over time, while camera-based maps can be more detailed visually, but may require more processing to handle changing conditions. Hybrid approaches that fuse LIDAR and cameras can deliver both high geometric accuracy and rich visual detail.

Other complex and costly alternatives are Laser tracker or Indoor GPS. There are cheaper and less complex technologies like Bluetooth Low Energy (BLE) and Ultra-Wideband (UWB). A summary of the different positioning systems evaluation can be found in Table 2-8.

Table 2-8: Position system evaluation regarding accuracy, complexity and cost

	ACCURACY	COMPLEXITY	COST
OPTICAL SYSTEMS			
LASER TRACKER	0.095 mm	High	High
OPTITRACK	0.1-0.5 mm	Medium/High	High
LIDAR	centimeters	Medium/High	Medium
RADIO-BASED SYSTEMS			
UWB, TDOA	50-100 cm	Medium	Low
BLE, RSSI-BASED	3 m	Low	Low
BLE, AOA	10-50 cm	Low	Low
5G LOCALIZATION, UTDOA	1-3 m	Medium/Low	None, *)

*) Comes with communication system

Except for Laser tracker all technologies support multi-target-tracking.

2.3.2 3GPP GNSS-RTK

2.3.2.1 Technical realization

As described in Deliverable 4.3. [19], in the Third Generation Partnership Project (3GPP) Release 15, transmission of RTK information through cellular telecommunication technologies was standardized [20]. The Secure User Plane Location (SUPL) standardized by the Open Mobile Alliance (OMA) is used for that.

RTK information is typically valid for areas of a few kilometers and changes in timescales of few seconds. According to the 3GPP-standardized procedures and architecture [21], it can be delivered over-the-top with no special cellular network features available besides the modem being capable of extracting network identifiers like the Tracking Area Code (TAC) or the Cell ID. When integrated with the Core network, the Mobility Management Entity (MME) in 5G NSA or Access and Mobility Management Function (AMF) in 5G SA provide this information to the location server. The end-device does not need to extract and send it. This reduces uplink data volume and, in many jurisdictions, means that user consent is required for collecting privacy-relevant information. The third variant broadcasts RTK correction data relevant for a given area within RAN System Information Blocks (SIB). The RTK correction data can be encrypted, so only users subscribed to the service will get the keys to decrypt it. This procedure is also standardized by 3GPP [21]. In Figure 2-22, a simplified 3GPP-

GNSS-RTK architecture is described to illustrate how the RTK data is broadcasted through the 5G network from the Internet to a 5G connected car.

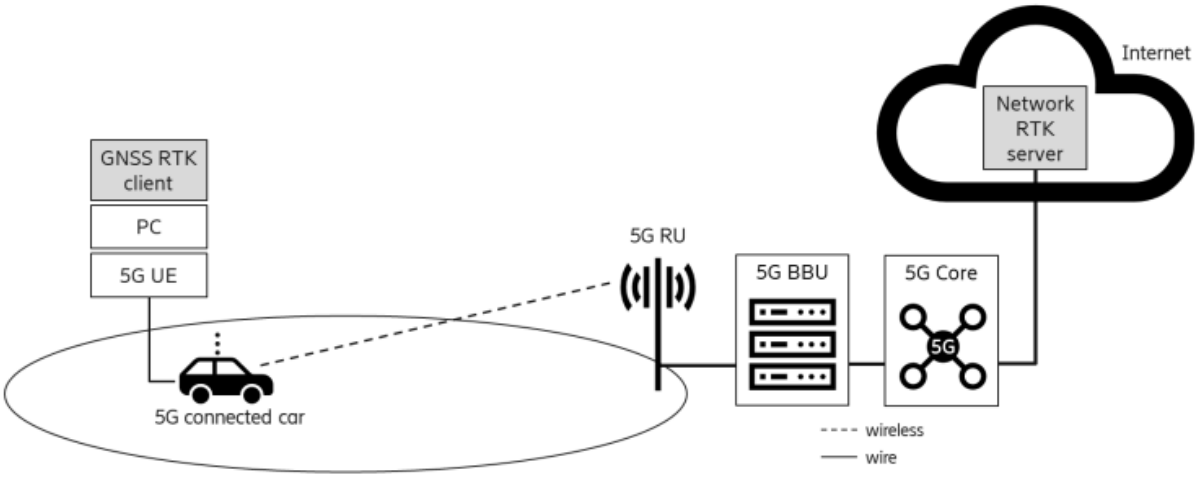

Figure 2-22: Simplified 3GPP-GNSS-RTK architecture

In our evaluation, a trial device is equipped with a Quectel R500Q 5G modem, a PC, a U-blox F9P GNSS receiver [22], and a GNSS antenna mounted on top of the vehicle. The modem provides 5G connectivity, while the PC injects the received RTK correction data into the GNSS receiver, where the GNSS receiver firmware uses it to improve the accuracy of the plain GNSS position.

The 3GPP Gateway Mobile Location Centre (GMLC) provides location information access to clients and applications, typically via a 3GPP NEF or an API gateway, but can be accessed directly when within a secure environment. GMLC provides location information combined with detailed uncertainty estimates on demand or as a periodic subscription. It can provide a network-based location information (subject to a reliable location request) or forward a device-reported location information. Within TARGET-X we used an GMLC prototype deployed in Sweden, accessible also from IDIADA. It is a prototype of Ericsson's commercial Ericsson Network Location product. It provided GNSS RTK correction information to end-devices and received device-reported information.

2.3.2.2 Evaluation

We conducted experiments at the 5G Industry Campus Europe (ICE) to analyze the precision of 3GPP-GNSS-RTK positioning in various scenarios. Initially, we evaluated the relative position error based on longitude and latitude during a static test, as shown in Figure 2-23(a). As the vehicle did not move, the position should also not change in the ideal case. Any "movement" is therefore the result of effects creating noise in the obtained GNSS position. We had no means in place to determine the true position. It is assumed as the mean value of the measured latitude and longitude. We converted the geodetic data (longitude and latitude) into Cartesian coordinates centered around the assumed true position. We fit the distribution of the coordinates into a normal distribution for each horizontal direction and calculated the mean (mu) and standard deviation (sigma) values. Altitude is not considered in this evaluation and assumed 0 m. In Figure 2-23(b) and Figure 2-23(c), the normal

distribution of the latitude and longitude coordinates indicates a sigma of ±25.50 mm and ±10.38 mm, respectively.

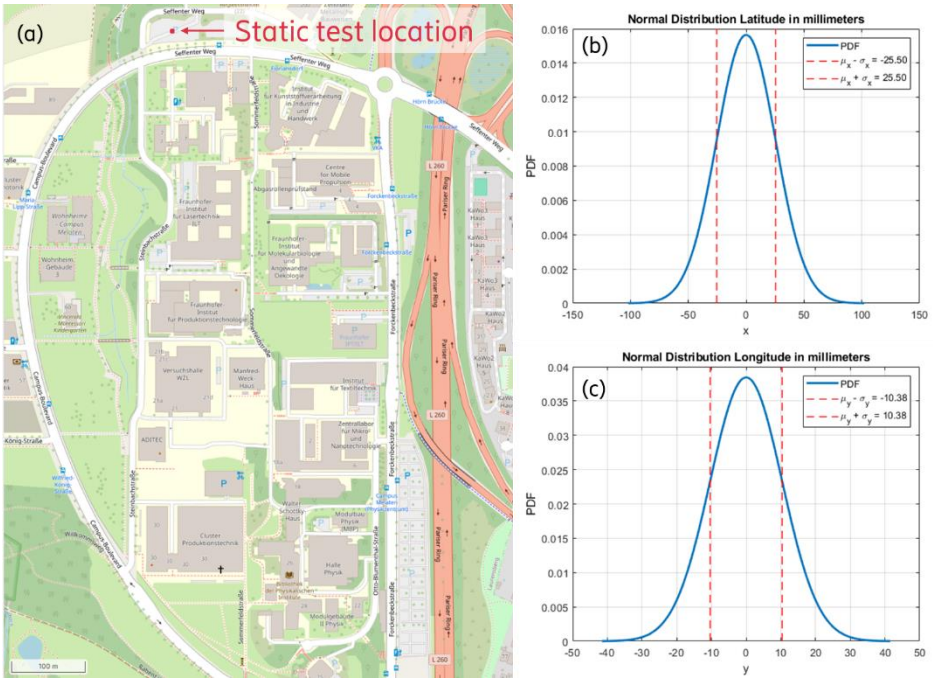

Figure 2-23: Position of the static test in the 5G Industry Campus Europe (a) and the normal distributions with same distribution as collected latitude (b) and longitude (c) samples in millimeters.

Another set of experiments involved a vehicle driving around the 5G ICE. In Figure 2-24(a), the vehicle completes laps with a direct view of the sky. In Figure 2-24(b), the vehicle follows a route near the 5G ICE, passing through obstructed areas, including four different bridges and a tunnel. A good GNSS signal, mostly related to the number of considered satellites, is a prerequisite for RTK correction to work. In case of bad GNSS signal or no RTK data coming from the Internet, the GNSS module reports "No RTK". In our case it only happened as a result of bad GNSS signal, as Internet connectivity through 5G was always assured. In case of impaired GNSS signal quality, the GNSS module reports "RTK float", meaning that the full potential of RTK correction is not being exploited. "RTK fix" indicates good GNSS signal quality and RTK correction being fully exploited. As shown in Figure 2-24, areas with a clear view of the sky achieve RTK fix positioning, while obstructed areas switch to "RTK float" and eventually "no RTK".

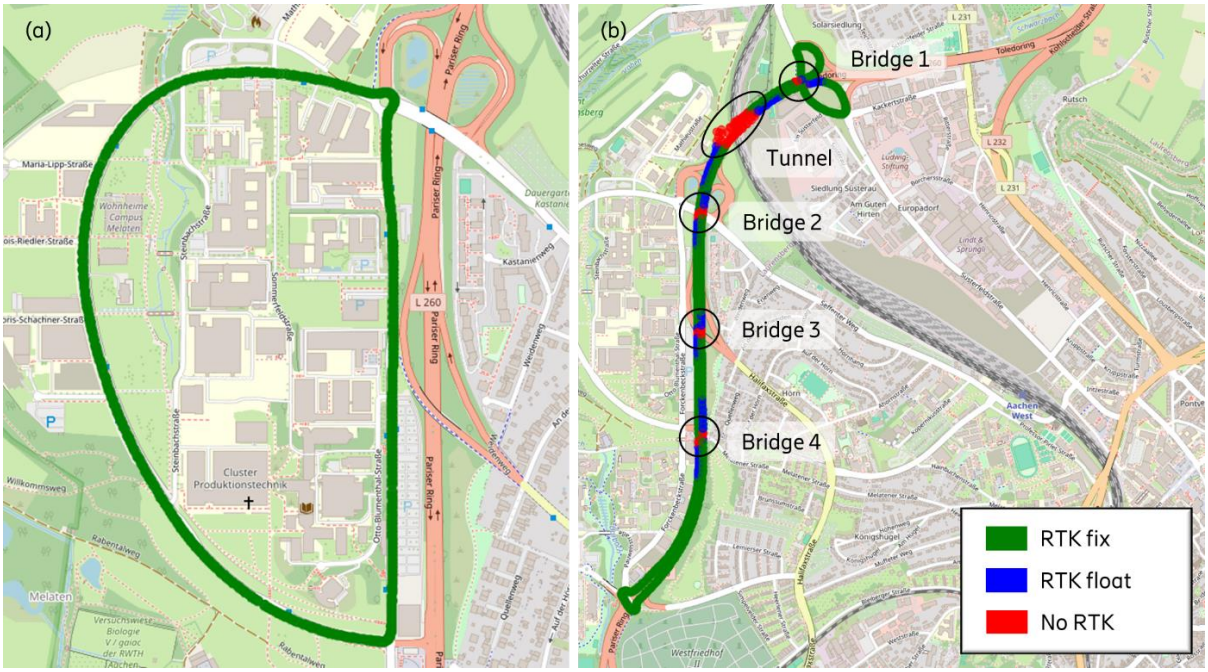

Figure 2-24: Type of RTK positioning accuracy for two mobile experiments in the 5G Industry Campus Europe.

Specifically, the position accuracy of the GNSS-RTK module under a tunnel is shown in Figure 2-25. Inside the tunnel, RTK positioning is lost, and location accuracy ranges from a few meters up to 21 meters. Similarly, when the device exits the tunnel (in both directions), RTK positioning improves to RTK float type, eventually achieving centimeter accuracy once the vehicle has a clear view of the sky.

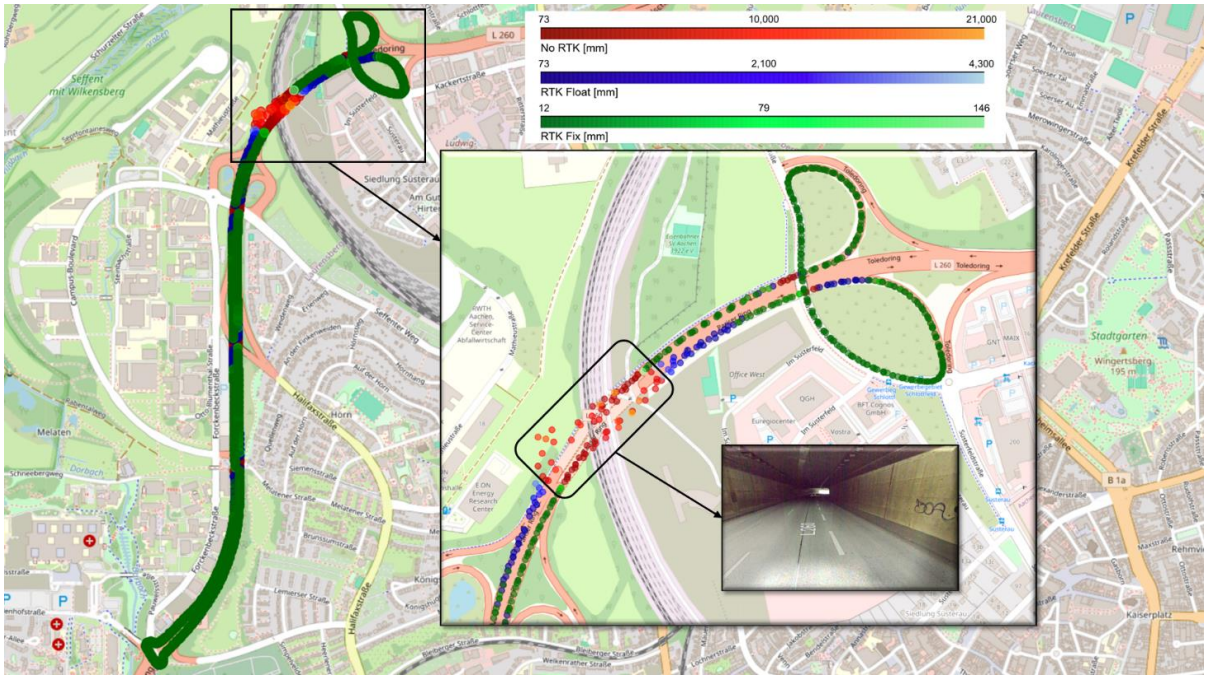

Figure 2-25: Accuracy values for a driving test going under 4 bridges and through a tunnel.

2.4 Real-time communication

2.4.1 Motivation for introduction

Wireless communication undergoes variable delays owing to packet retransmissions, processing delays at the terminal device as well as the network infrastructure, protocol stack signaling, alignment delays with respect to the packet transmit opportunity, etc. Such variable delays are not desirable for realtime applications.

In the TARGET-X project, we empirically evaluated redundant 5G transmissions using the FRER (Frame Replication and Elimination for Reliability) protocol. FRER has two main functions: replication and elimination. The FRER protocol sends frames after replication on multiple disjoint paths. The elimination function deletes any redundant frames received. Our empirical study on the use of FRER with 5G transmissions highlights that packet delay variations are reduced thereby making transmissions more robust and suitable to realtime applications.

2.4.2 Technical realization

We carried out comprehensive 5G-FRER over-the-air measurements in an industrial environment involving multiple UEs on the same and different 5G systems. The results have been reported in a TARGET-X journal paper contribution [23]. The 5G systems used in this study include the following:

- 5G Midband System (3.7–3.8 GHz): A locally licensed 5G n78 system with 100 MHz bandwidth, offering excellent factory-wide coverage and reliable non-line-of-sight (NLOS) propagation for industrial shop floors.
- 5G mmWave System (26 GHz): A 5G n258 system with 800 MHz bandwidth, suitable for low-mobility, high-data-rate applications, utilizing beamforming to overcome the higher path loss associated with mmWave frequencies.
- 5G URLLC Test System (28 GHz): A pre-commercial standalone test system compliant with 3GPP Release 16/17, leveraging ultra-reliable low-latency communication features, including Ethernet PDU sessions and QoS mapping, to meet stringent application requirements.

The FRER implementation is based on commercial off the shelf TSN switches from Moxa Inc. In our tests, we mainly focused on two redundant paths as redundancy comes with the cost of additional radio resource consumption. While native Layer-2 support was not available in the commercially available 5G equipment at the time of empirical testing, we used Layer-2 tunneling. The technical realization is based on the three main setups as shown in Figure 2-26. For further details, please see our paper [23].

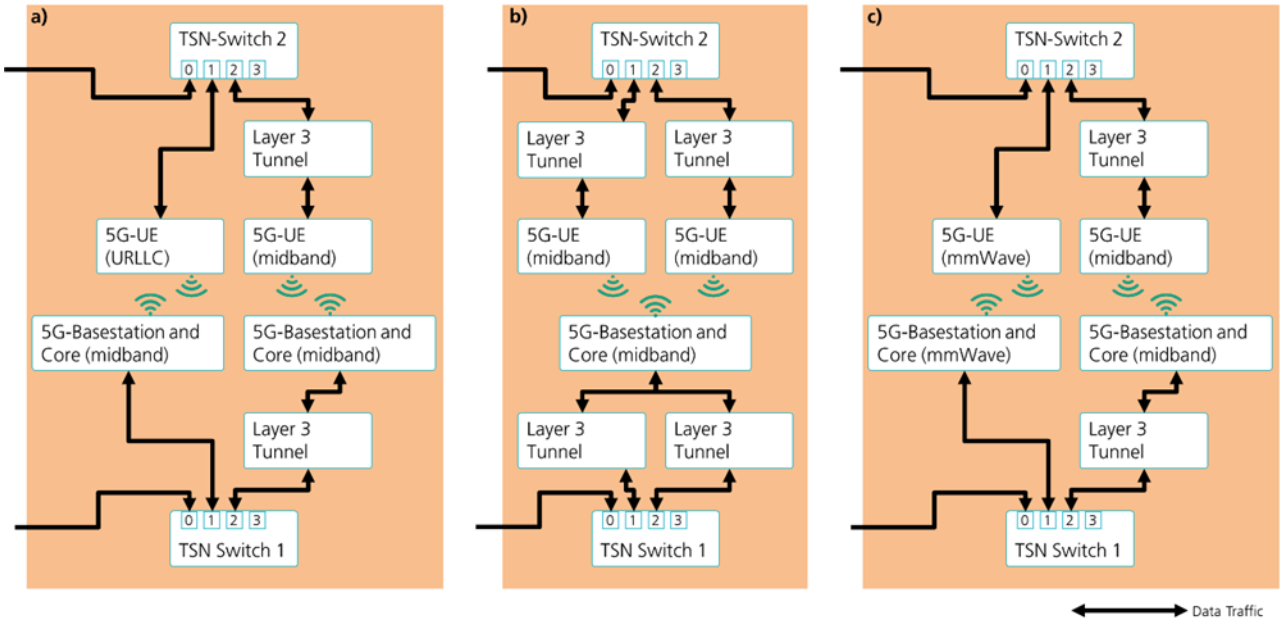

Figure 2-26: a) Using FRER for redundant transmission in the 5G midband and URLLC testbed deployment. b) FRER setup for redundant transmissions with multiple UEs in the 5G midband system. c) Using FRER for redundant transmission in the 5G midband and 5G mmWave system

2.4.3 Evaluation

The evaluation was carried out at the shopfloor of the Fraunhofer IPT at the 5G-Industry Campus Europe in Aachen with an industrial environment. The three setups as in Figure 2-26 were used in mainly five different evaluation scenarios as described below. Please note that the evaluation requirements have been derived from manufacturing use-cases of TARGET-X as reported in [24].

Test 1: Redundant transmissions using the same 5G Midband System in Setup b)

Data packets were replicated and transmitted via multiple User Equipment (UE) devices on the same 5G midband network (3.7–3.8 GHz). Data packets were sent through a TSN network, replicated at the sender, and transmitted through separate UEs. At the receiver's end, redundant packets were eliminated, and the first correctly received copy was used for further processing. The goal was to observe improvements in reliability and reduction in latency within the same network. The results shown in Table 2-9 indicate that none of the two communication paths achieved the required 10 ms latency bound target for 99.99-th percentile, but after combining the redundant streams on Switch 1 (overall), an average latency of 8.28 ms could be observed. This showcases how FRER can increase reliability with using one network with multiple UEs.

Test 2: Redundant transmissions using two separate 5G Midband Systems in Setup b)

This configuration extended Test 1 by using two separate midband 5G systems, one NSA (non-standalone) and one SA. The two systems operated in parallel, ensuring that packet delivery was not affected by failures or interference in one of the systems. The results shown in Table 2-9 indicate again, that none of the two communication paths achieved the required 10 ms for 99.99% of the messages, but after combining the redundant streams on Switch 1 (overall), an average latency of 8.43 ms could be observed.

Test 3: Using 5G URLLC Test System in parallel to 5G Midband in Setup a)

This setup tested the pre-commercial 5G URLLC system (28 GHz) with layer 2 support in parallel with a commercially available midband system. The URLLC Test System supported advanced features such as over-the-air time synchronization, Ethernet PDU sessions, and traffic prioritization. The results shown in Table 2-9 show, that the URLLC Test System outperforms the midband system, therefore FRER has no impact on the overall performance of the setup.

Test 4: Parallel use of 5G Midband and mmWave Systems in Setup c)

In this setup, data packets were transmitted redundantly using two different types of 5G systems: a midband system (3.7–3.8 GHz) and a mmWave system (26 GHz). The trial aimed to understand the benefits of combining two systems with different propagation characteristics, bandwidths, and susceptibilities to environmental factors. The results shown in Table 2-9 indicate that the high performance of the mmWave system achieved the required 10 ms for 99.99% of the messages, and the combination of the redundant streams on Switch 1 (overall), improved the average latency only by 0.02 ms.

Test 5: Parallel use of 5G Midband and mmWave Systems in Setup c) with disturbances

In this setup, the focus was on testing the combination of midband and mmWave under the presence of intentional disturbances to assess the communication system's resilience, reliability, and latency in an industrial environment. To create the disturbances, a metal panel was placed in front of the mmWave device to simulate line-of-sight (LOS) blockages. This reflected real-world scenarios where tools, equipment, or workers may obstruct high-frequency signals, which are particularly sensitive to such conditions. The results shown in Table 2-9 indicate that due to the blockage, the performance of the mmWave Path dropped to 27.49 ms, therefore did not achieve the required 10 ms for 99.99% of the messages. But after combining the redundant streams on Switch 1 (overall) , an average latency of 9.24 ms could be observed.

Table 2-9: Evaluation results of the 5G-FRER testing in various scenarios.

Setup	Path 1 99.99% Latency	Path 2 99.99% Latency	Overall 99.99% Latency
midband NSA + midband NSA	11.16 ms	10.95 ms	8.28 ms
midband NSA + midband SA	11.46 ms	18.78 ms	8.43 ms
midband SA + midband URLLC	11.83 ms	1.09 ms	1.09 ms
midband NSA + mmWave NSA	12.30 ms	6.31 ms	6.29 ms
midband SA + mmWave NSA with induced disturbances	11.64 ms	27.49 ms	9.24 ms

The results highlight that FRER improves reliability of 5G transmissions and as a side effect reduces the overall latency.

Besides the use of FRER for reliability improvements, we have carried out Radio Access Network (RAN) configuration parameter selection in a manner that better supports the requirements of realtime applications, i.e., enhancing reliability and reducing the communication latency. One such example is our TARGET-X work on the evaluation of mmWave communication for manufacturing use-cases at Fraunhofer IPT shopfloor [13]. In this work, we explored, in particular, the suitable Time Division Duplexing (TDD) patterns that support the application traffic profiles in the uplink and downlink directions and the selection of Block Error Rate (BLER) target. Our empirical results quantify the gains for different uplink and the downlink traffic profiles with different TDD patterns – naturally, uplink transmissions benefit from higher number of uplink slots in a TDD pattern and vice-versa for the downlink traffic. Our experimental results highlight that lower BLER targets while making mmWave transmissions more robust against signal outages especially in non-line-of-sight and occluded line-of-sight scenarios, larger coding overhead associated with lower BLER targets has the side effect of lower achievable peak throughput.

2.5 Asset Administration Shell

2.5.1 Motivation for introduction

Next generation industries are expected to have advanced communication requirements which can be addressed with the advances in telecommunication technologies such as 5G and beyond networks. The motivation that leads to the development of 5G networks are to address these specific requirements coming from the I4.0 verticals. These mainly focus on automation of network operations and practical and fast configuration for efficient use of resources. However, this capability requires 5G networks to be integrated with the industry domain. However, the complex nature of telco networks highly limits the interaction of the communication systems to the external applications. Moreover, industrial devices are not designed to interact with the 5G NW exposures by default. Digital twin and industrial integration technologies play a pivotal role in overcoming such challenges. To have an abstraction layer that enables interoperability across different verticals and multi-vendor environments, there is a need to have standardized tools for exposures. One promising solution for this challenge is Asset Administration Shell (AAS), which creates the digital twin (DT) of the industrial assets. Since a 5G NPN is also an industrial asset on the factory floor, representation of the 5G network in the form of AAS is the key for seamless interoperability between assets' digital twins, and consequently, between physical assets, including the 5G NPN.

2.5.2 Technical realization

Asset Administration Shell is highly adopted by smart industries. Many industrial device manufacturers are providing their devices' AAS bundled with the delivery.

The basic setup that can be used in a typical deployment environment consists of an AAS Server, AAS Registry and AAS of the assets, such as 5G NW AAS and 5G UE AAS. AAS Server needs to be deployed in a VM that can be reached by the services that make use of AAS REST APIs.

To fill the AAS submodel elements, EP5G [3], TS29.435 [25], TS29.564 [26], TS29.572 [27], TS29.520 [28], Analytics exposure, SMF PDU and CAMARA Quality on demand [29] exposures are utilized. While EP5G is available in the deployment environment, others were not available, thus they are provided via mock services. These mock services are consumable via REST APIs. For this, producer services are obtaining information from both EP5G APIs and mock services' APIs and continuously updating the AAS on the AAS server.

The UE AAS has been implemented through a UE developed by Fivecomm, which consists of a 5G HAT including the 5G module RG520N from Quectel (5G Release-16 compatible) and a Raspberry Pi 4 implementing the Linux distribution OpenWRT [30]. On the Raspberry Pi, a Python script for updating the AAS is executed and later the AAS is updated in the server via an HTTP command. The update interval can be chosen depending on the needs of the specific use case. In this scenario, we implemented an update in the UE AAS every 1 minute.

A more detailed description of the 5G NW AAS, 5G UE AAS and implementation can be found in the corresponding deliverables [31], [32].

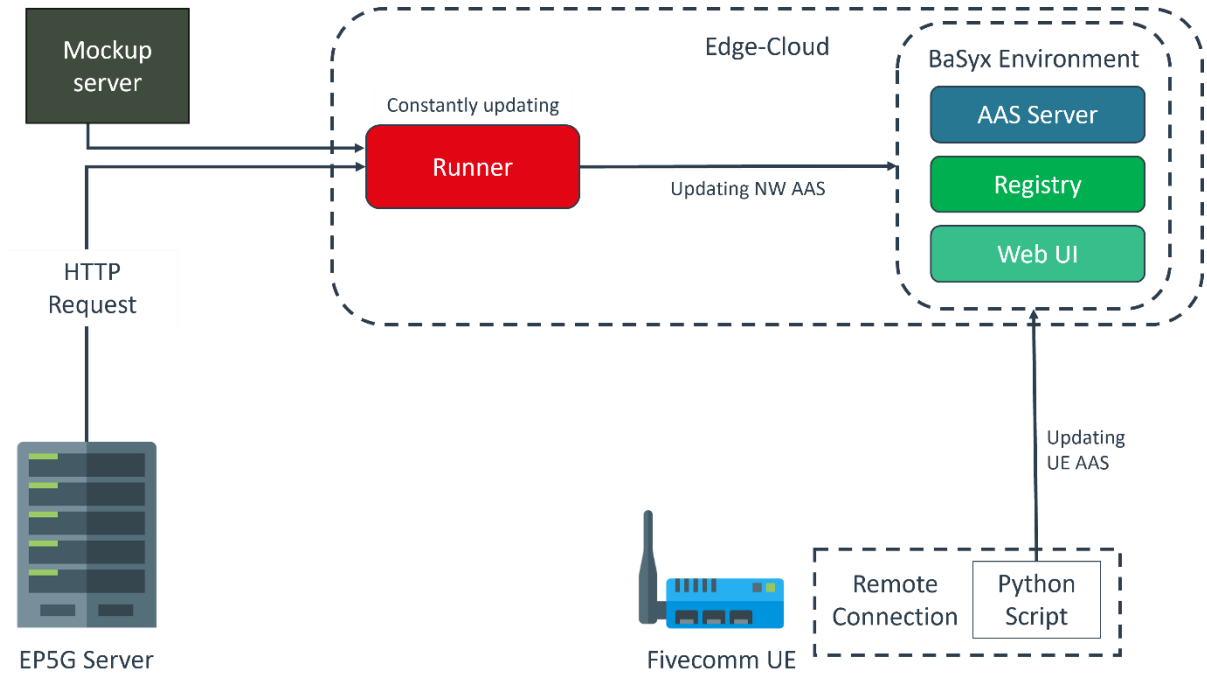

Figure 2-27: AAS realization setup

2.5.3 Evaluation

To evaluate the setup, we implement an application that makes use of the information provided by the AAS to bring the application domain and the telecommunication domain closer together.

Traffic steering demo

Traffic steering refers to choosing the carrier / route the traffic should take. With getting information from the network AAS about the UL load, it is possible to do traffic steering on the application level. On the shopfloor at IPT, we receive information about the network uplink load in the AAS. Using this information, we implemented a simple traffic steering demonstrator. We use two devices that compete for network resources:

- Fivecomm UE sending iperf traffic to load the network
- A midband and mmWave capable UE uploading a video

With a network monitoring script, we check the midband uplink load, and once it crosses a certain threshold, we check based on information in the AAS if one of the devices in the network is mmWave capable. We then signal the mmWave capable device to change the band towards the mmWave. In the following, we can watch the midband load reduce and the band of the mmWave capable device change to n257.

With this setup, we use this newly available information from the AAS to have an informed application influence the network load, thus, integrating the application domain and the telecommunication domain.

2.6 Far-edge / Edge Continuum

2.6.1 Motivation for introduction

The far-edge/edge continuum solution for remote power consumption monitoring tool is an inter-vertical collaboration that is handled through WP6. The idea had been employing the VILLAS framework, which is introduced in Deliverable 3.4 [33], to monitor power consumption of electric vehicles and record statistics and generate consumption models.

The VILLAS framework [34] is an open-source software set with different components that allows to collect power consumption KPIs from the connected devices and provide further assessment [33]. The idea of integrating VILLAS nodes in a vehicle is introduced in Deliverable 4.3 [19] and the technical details about how to develop relevant functions are explained in this document.

2.6.2 Technical realization

The VILLAS solution relies on VILLASnodes, which are developed in containers (see Figure XX). The VILLASnode1 receives analog energy metrics as input and timestamps them. There is no limit for the input sample rate while the common sample rate is from some hundreds up to hundres of kilo samples per second. The VILLASnode2 hosts the Dynamic phasor conversion (DFT) algorithm to perform phasor estimation. The DFT converts thousands of samples received into a few average samples as the indicator of the consumption trend. The concluded results will be further plotted in Grafana for administrative purposes.

The motivation for proposing far-edge/edge continuum solution is that the DFT is a compute-hungry process, hence better to offload it to the edge. However, in the automotive use cases and since the vehicle is moving around receiving different network connectivity qualities, it will be very likely that network resources won't be enough to send raw data from VILLASnode1 to VILLASnode2. In this case, it is essential to run VILLASnode2 in the vehicle as well and only send concluded short data to Grafana, hence saving network resources. So, the key innovation will be considering a trade-off between available network resources and remaining power in the vehicle.

Figure 2-28 depicts the architecture and functions to collect and store power consumption metrics. The blue border functions are basic functions developed in the structure of WP3 and reported in deliverable D3.4[33] . The red border and green function are the features that are added to the solution to adapt it to far-edge/edge continuum scenario to be used in a vehicle.

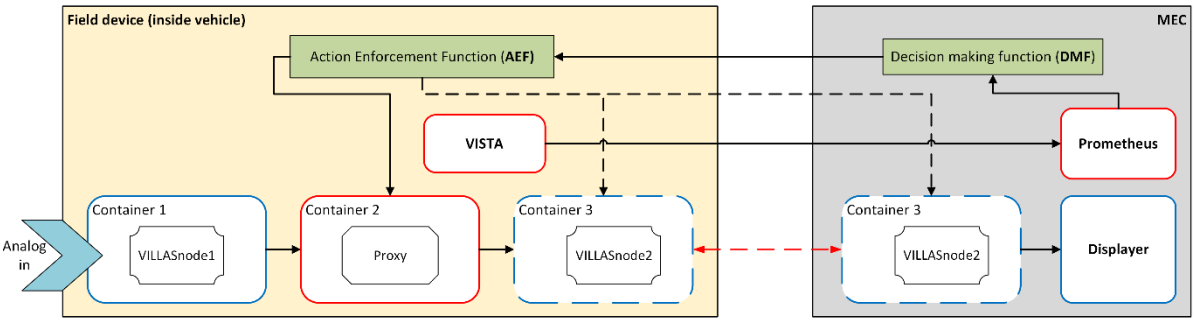

Figure 2-28: VILLASframework integration into vehicle

In the initial deployment in WP3, container 3 in Figure 2-28 was always running in the MEC server whereas in the framework of the far-edge/edge continuum, it is considered to dynamically move it from MEC to the field device. The Decision-Making Function (DMF) assesses network KPIs and decides whether container 3 should stay running on the MEC or should be moved to the device inside the vehicle. DMF relies on connectivity quality that is reported by VISTA. Once the decision is made by DMF to move the VILLASnode2 (i.e. container3) to vehicle, an event will be triggered by Action Enforcement Function (AEF) to create and run the container inside the vehicle and send its outputs to the displayer on the edge. The functionality of container2 in Figure 2-28 is to facilitate development by abstracting container1 development network configuration from complexity of container3 movement.

Figure 2-29 is an example of the running system when container3 is running on the edge (top part of the figure) and container1 is running in the vehicle device (bottom part of the figure).

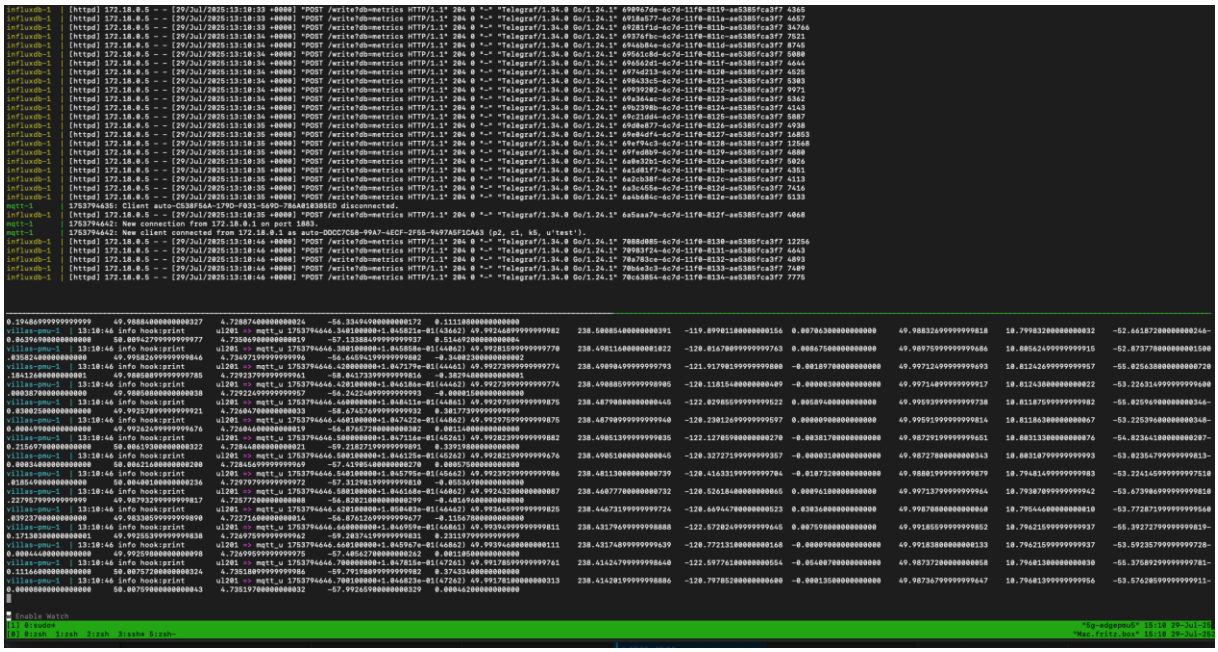

Figure 2-29: VILLASframework when the VILLASnode1 in running in the vehicle (bottom part) and VILLASnode2 is running on the edge server (upper part)

Figure 2-30 shows the displayer console that is running on the edge reporting power consumption metrics. In this PoC to validate the solution, the consumption of a laptop inside the vehicle that consumes 220V power is measured.

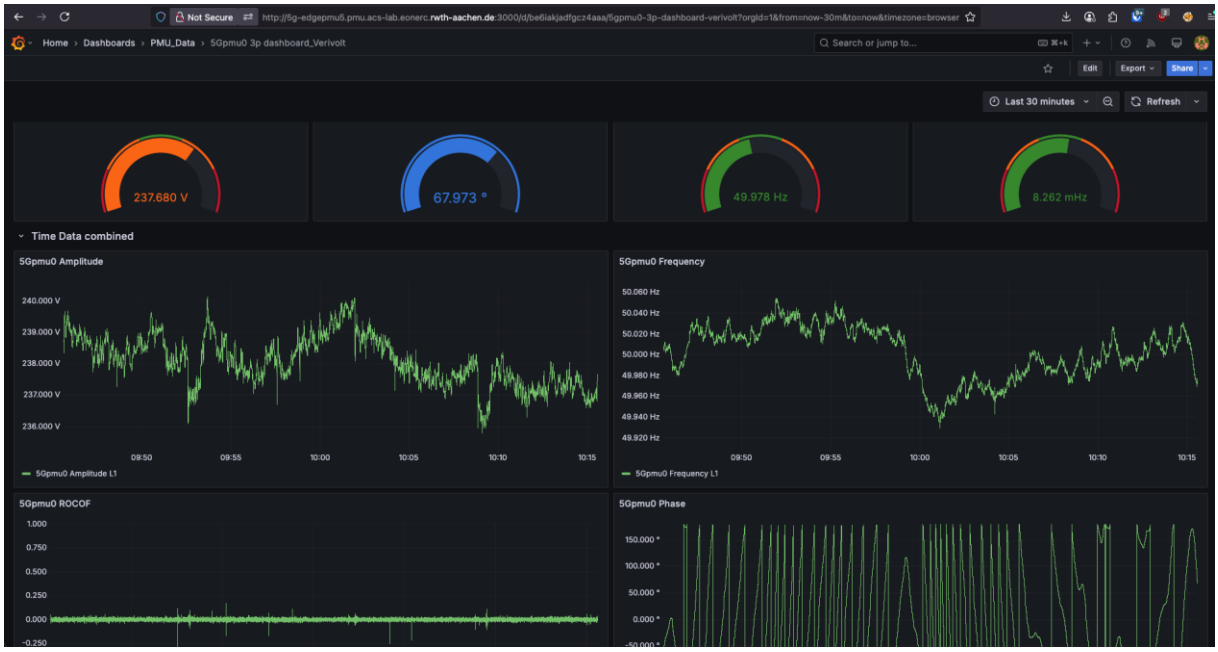

Figure 2-30: Displayer dashboard to report collected power consumption metrics

2.6.3 Evaluation

Devices that are shown in Figure 2-31 are employed to validate the solution. The devices on the left side (i.e. Figure 2-31 a) are Measurement Head that receive analog power as input and send them for further processes. The first one has a socket of AC power, and the second one is adapted for 12V DC car sockets.

The device on the right side (i.e. figure Figure 2-31b) is the edgePMU that includes a small pc (i.e. a Raspberry Pi), GPS antenna and 5G module. The small PC is to host VILLASnodes and relevant functions.

a: Measurement heads

b: edgePMU

Figure 2-31: VILLASnodes that are used for the validation setup

Following the architecture that is depicted in Figure 2-28, we observed a considerable decrement in network resource consumption when container 3 is executing in the field device. Figure 2-32 shows that communication between container1 and container 3 is 4.01 Mbps when container 3 is running on the edge while this throughput decreases to 166.10 Kbps when container 3 is running in the field device close to container 1 and only sends the phase estimation results (Please see Figure 2-33). It is worth mentioning again that this network resource decrement is in the cost of dramatically increasing computation resources in the field device, hence consuming more power in the vehicle.

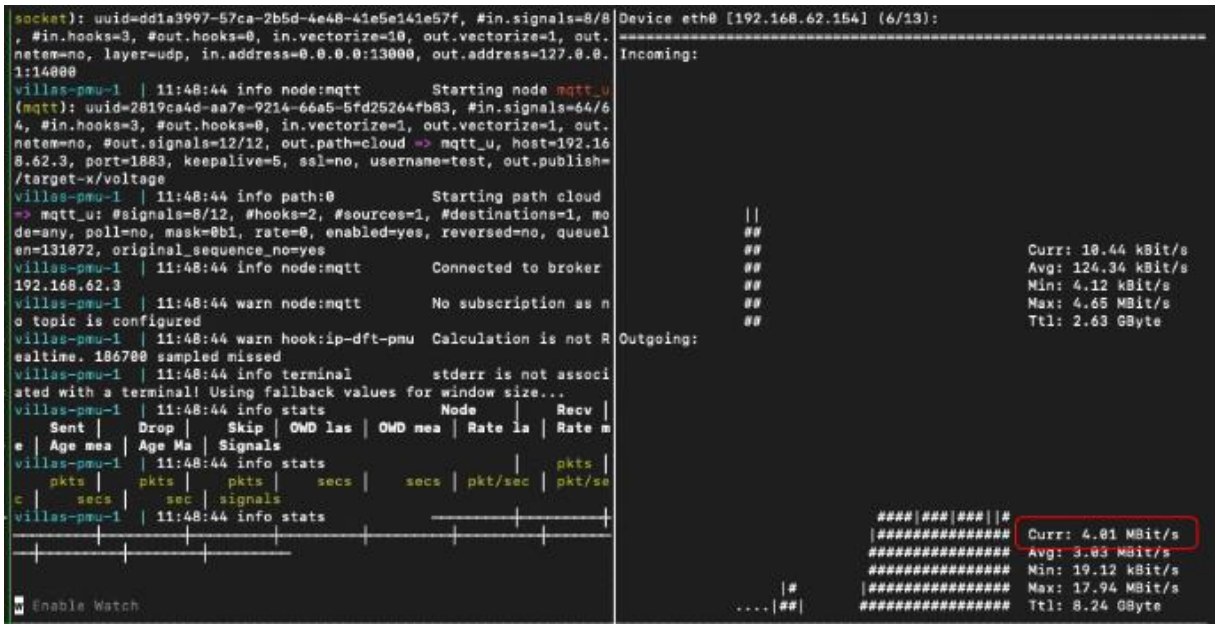

Figure 2-32: Network resource consumption when container 3 is running on the edge.

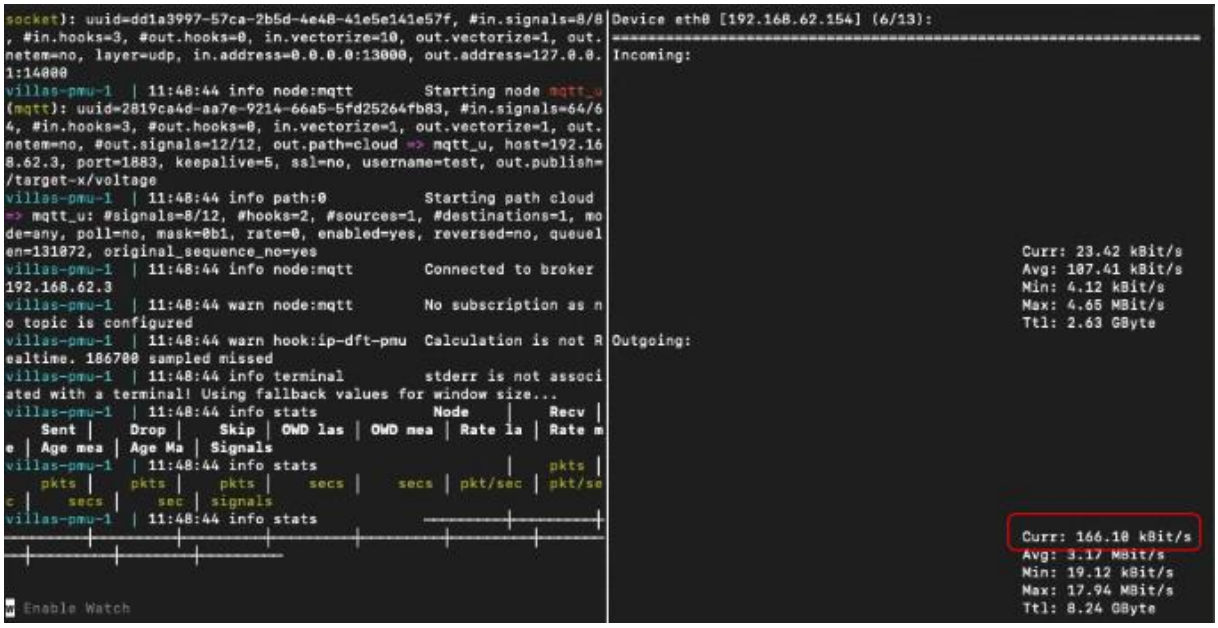

Figure 2-33: Network resource consumption when container 3 is running in the field device.

2.7 RedCap

2.7.1 Motivation for introduction

RedCap (Reduced Capability) devices, as introduced with 3GPP Release 17, brings new and interesting features to the device ecosystem in the industrial verticals served by TARGET-X. The introduction of RedCap was not planned in the early phases of the project, but as the functionality became available, both in RAN and on the device side, a brief evaluation of RedCap was deemed to be an interesting addition to the technology bricks that were introduced and evaluated within the project.

RedCap devices are designed with fewer RF chains, a simpler baseband and reduced feature sets. The simpler design reduces the complexity, and thus also the cost per device, compared to regular 5G devices and thus providing a large class of lower-cost, lower-power, simpler cellular IoT devices that still benefit from 5G coverage, security and manageability while reducing device and operational costs. The Figure 2-34 below illustrates the comparison of the different 5G NR classes with regards to data rates, latency and cost combined with battery life, with RedCap having a significant performance in all aspects, without excelling in any of the KPIs. A more detailed description of RedCap and the achievable KPIs can be found in the Ericsson whitepaper [35].

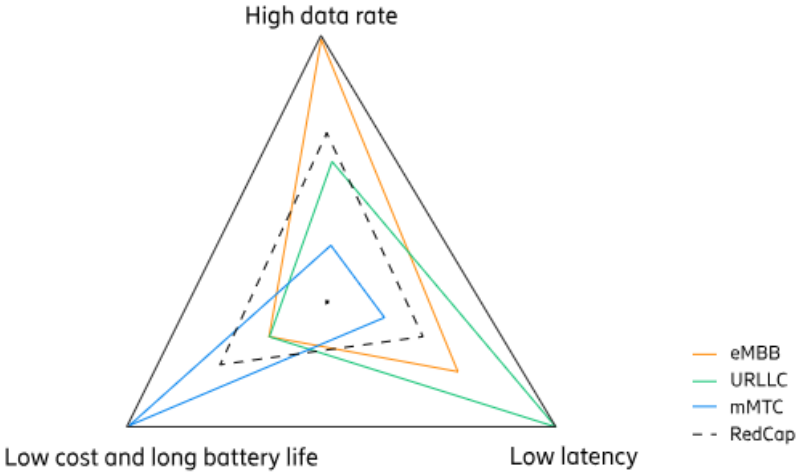

Figure 2-34: KPI comparison chart between 5G NR devices classes (Ericsson whitepaper)

A practical evaluation of RedCap with regards to achievable latency and throughput, as well as measurements of power consumption were deemed to be feasible within the runtime of the project.

2.7.2 Technical realization

A precondition for the introduction of RedCap is to have a 5G NR SA network available, as RedCap is an SA-only feature. The IPT shopfloor was chosen for the initial activation of RedCap, as the SA architecture was available, and with the wireless sensor platform, offers a matching use case class for use of RedCap modules.

An approach to limit RedCap introduction to a single cell was selected to limit the configuration efforts, and to have faster availability of the RedCap feature for testing.

While regular devices continued to have access to the full 100 MHz of midband industry spectrum, the RedCap devices, as per specification, only had access to 20 MHz, as depicted in Figure 2-35.

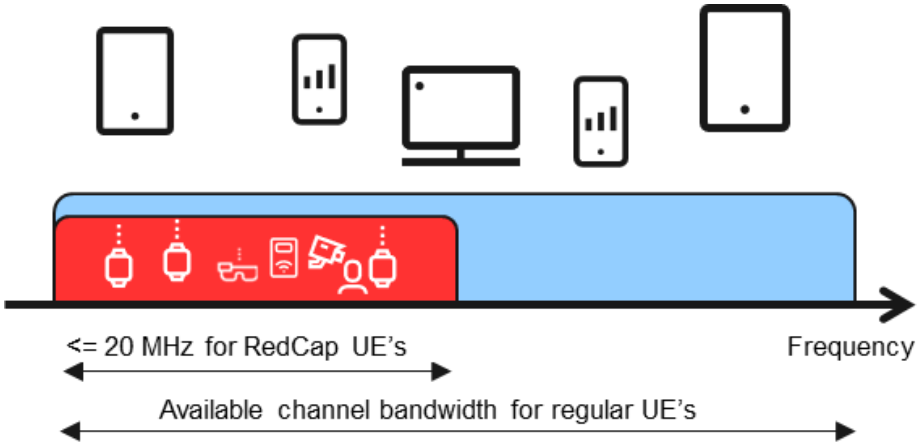

Figure 2-35: Spectrum availability for RedCap vs. regular 5G devices

DRX (Discontinuous Reception) where the radio periodically wakes to check for downlink paging or data. Regular DRX cycles are short so the network can reach the device quickly and eDRX (extended DRX), a configurable mode where DRX cycles are lengthened (minutes rather than seconds), so the device checks in much less frequently and consumes less power, were disabled to create similar conditions for both device types.

2.7.3 Evaluation

The practical evaluation of RedCap versus regular modules was performed as part of evaluation activities, executed together with WP2, the work package in TARGET focusing on manufacturing use cases.

The detailed description of the execution environment and the obtained results are documented in Deliverable D2.5 [24].

3 Large-scale trial

3.1 Setup of the large-scale trial

For the detailed evaluation and validation of 5G network performance under realistic industrial load conditions the PRISM Monitoring System (Performance & Reliability Insight System for Mobile Networks) was developed and utilized at Fraunhofer IPT's shopfloor at 5G-Industry Campus Europe. The PRISM Monitoring System enables coordinated measurements and analysis of various 5G technologies, such as sub6, RedCap or mmWave, in industrial campus networks.

3.1.1 Hardware

All trials are conducted at the 5G-Industry Campus Europe in Aachen, Germany. This unique research infrastructure provides a 5G campus network, covering both indoor and outdoor areas. The network is fully equipped with a 5G-SA and NSA architecture, supporting both sub6 GHz (FR1) and millimeter-wave (FR2) frequency bands, making it an ideal environment for testing industrial use cases.

The core measurement setup is the custom-developed PRISM (Performance & Reliability Insight System for Mobile Networks) monitoring tool. Its hardware consists of:

- Central Control Unit: A high-performance mini-PC (in this case LattePanda Sigma) serves as the central orchestration and data analysis hub. It hosts the graphical user interface and the primary test logic.
- Sensor nodes: A distributed network of up to 60 dedicated sensor nodes, based on Raspberry Pi 5 single-board computers is deployed across the network. Each node is equipped with a specific 5G modem of a distinct device class.
- Test Server: A dedicated server within the campus network, identified by a certain IP address, acts as the central endpoint for throughput and latency measurements. This test server consists of multiple LattePanda Sigmas.

To simulate a realistic number of industrial IoT devices, the sensor nodes are equipped with three distinct classes of 5G modems:

- 60x sub6 GHz (FR1) devices - **Waveshare RM520N-GL 5G HAT:** The devices come with the Quectel RM520N-GL 5G Sub6 GHz module and supports various network standards, such as 5G/4G/3G or GNSS positioning. It can be directly connected and controlled via the Raspberry Pi 5 GPIO header.
- 40x RedCap (Reduced Capability) devices – **Teltonika RUT 976:** The device is an industrial grade RedCap 5G router, downwards compatible with 4G LTE. It is connected and controlled directly via the central control unit or, alternatively directly by the Raspberry Pi Sensor Nodes.
- 12x mmWave (FR2) devices – **Quectel 5G mmWave LP EVB Kit with RM530N-GL**: This device is a mmWave capable module, supporting n257, n258, n260 and n261. It supports mmWave NSA networks and therefore also sub6 GHz frequencies. It is controlled by the Raspberry Pi Sensor Nodes via USB.

3.1.2 Software modules and architecture

The 5G PRISM tool is built on a modular client-server architecture, designed for flexibility and scalability. The architecture is as follows:

The main application, running on the central control unit provides a comprehensive user interface for test configuration, live monitoring and result analysis. It functions as the orchestrator, initiating and managing all test campaigns across the distributed sensor node network.

Each sensor node runs a lightweight, autonomous script. This script acts as a server with two primary responsibilities:

- It directly interfaces with the connected 5G modem to collect radio-level data, including RSRP, SINR and others.
- It provides a simple HTTP API to serve the collected measurement data in JSON format and receive commands from the central control unit to trigger coordinated tests.

A key component of the central application is the result explorer. It processes the raw data generated during the campaign and automatically creates intuitive visualizations, such as Cumulative Distribution Functions, time-series graphs and more, to facilitate immediate analysis and interpretation of the results.

A scheme of the architecture is also given in Figure 3-1 below.

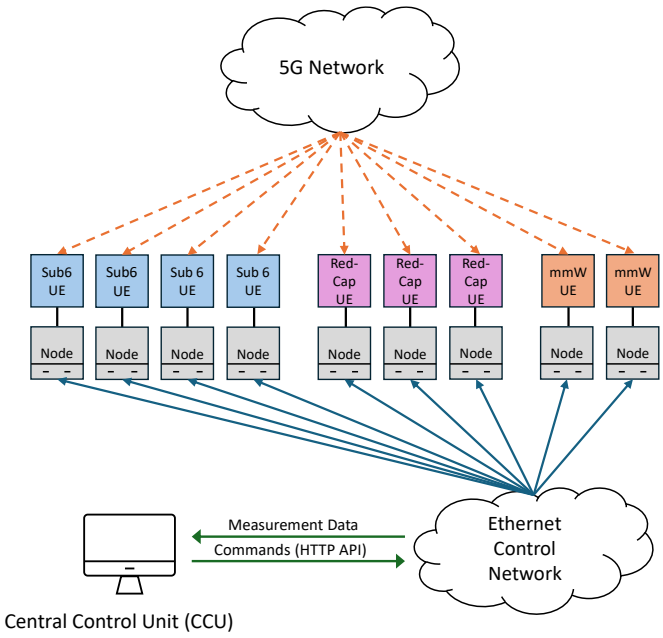

Figure 3-1: Architecture of the Measurement Software.

3.2 Description of planned test scenarios

The measurement campaign is structured into three primary scenarios. Each scenario is executed sequentially for each of the three device classes to obtain a differentiated view of the network performance.

3.2.1 Scenario 1: Single Node Baseline Performance

The objective is to establish an individual performance baseline for each of the sensor nodes in an isolated, non-congested state. This phase includes:

- Time-to-Attach Measurements: A critical industrial KPI is measured. For each node, the system quantifies the “network-login” attach time (radio on/off cycle).
- Maximum Throughput Test: Each node individually performs TCP and UDP throughput tests (uplink and downlink) against the central server to determine its maximum achievable data rate under ideal conditions.
- Latency & Jitter Measurements: A baseline test is conducted to measure the round trip time (RTT) and jitter in an unloaded network state to serve as a reference value.

3.2.2 Scenario 2: Coordinated Multi-Node Load Tests

This phase simulates realistic, large-scale network usage patterns by activating multiple sensor nodes simultaneously. The focus shifts to understanding how the 5Gnetwork behaves under aggregated load and how it manages network resources.

- Many-to-One Test (Converged Traffic): A large number of devices initiate a TCP upload to the central server at the exact same time. This scenario simulates use cases such as the simultaneous upload of video streams from multiple quality control cameras. Key metrics include the aggregated throughput of the cell and the individual throughput per device, which reveals the network’s strategy for managing resource contention.
- One-to-Many Test (Diverged Traffic): The central server simultaneously pushed data to a large number of devices. This simulated broadcast-like scenario, such as deploying a software update to many machines at once. Key metrics are individual receive rates, packet loss and jitter under load to assess the stability of the downlink distribution.

3.2.3 Scenario 3: Long-Term Stability & Reliability

The objective is to assess the network’s stability over extended periods. A coordinated traffic pattern, such as “Many-to-One” test is executed continuously at a moderate intensity over a 8-24 hour period. This long-duration test is designed to identify hard-to-diagnoses issues like slow performance degradation, memory leaks in network components or periodic interface patterns that might be missed in short-term tests.

3.3 Execution

In the following section, the execution and the results of the large-scale measurement campaign will be presented. The measurement campaign took place on the shopfloor at the Fraunhofer IPT in Aachen, part of the 5G-Industry Campus Europe.

3.3.1 Description of Execution Environment

The large-scale measurement campaign took place at the 5G-Industry Campus Europe, one of the TARGET-X testbeds. The 5G network at the Fraunhofer IPT features both 5G SA and NSA modes. While the mmWave measurements were conducted using the NSA mode, the sub-6 GHz and RedCap measurements were conducted in the SA mode.

The mmWave measurements took place in the n257 frequency band using the DDSUU TDD pattern. In this band, 800 MHz of bandwidth was utilized, which is divided into 8 carriers (Component Carriers) with a subcarrier spacing of 120 kHz. The mmWave network features two mmWave antennas placed in two corners of the shopfloor. This mounting location allows for good radio coverage in all aisles.

The sub-6 GHz and RedCap measurements were conducted in the n78 band, the standard band for private 5G networks in Germany, utilizing the 5G SA network. This SA network is established with 8 Radio Dots, providing good coverage across the entire shopfloor. While the standard sub-6 GHz measurements utilized 100 MHz of bandwidth, the RedCap measurements used only a portion of this, specifically 20 MHz.

To avoid mutual interference, the devices were distributed evenly across the shopfloor. The distribution along the shopfloor is shown in Figure 3-2 for the Sub-6 devices, in Figure 3-3 for the mmWave devices and in Figure 3-3 for the RedCap devices.

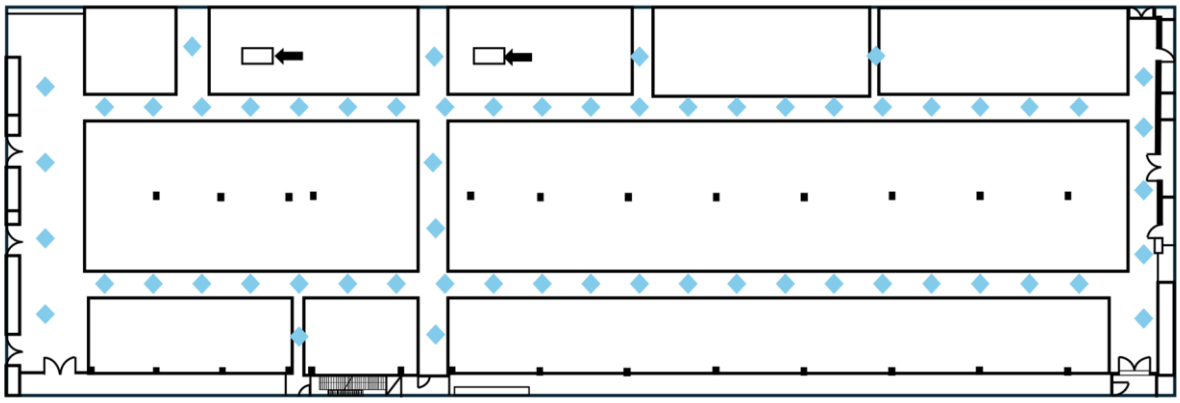

Figure 3-2: Distribution of the Sub-6 GHz Devices across the Fraunhofer IPT Shopfloor.

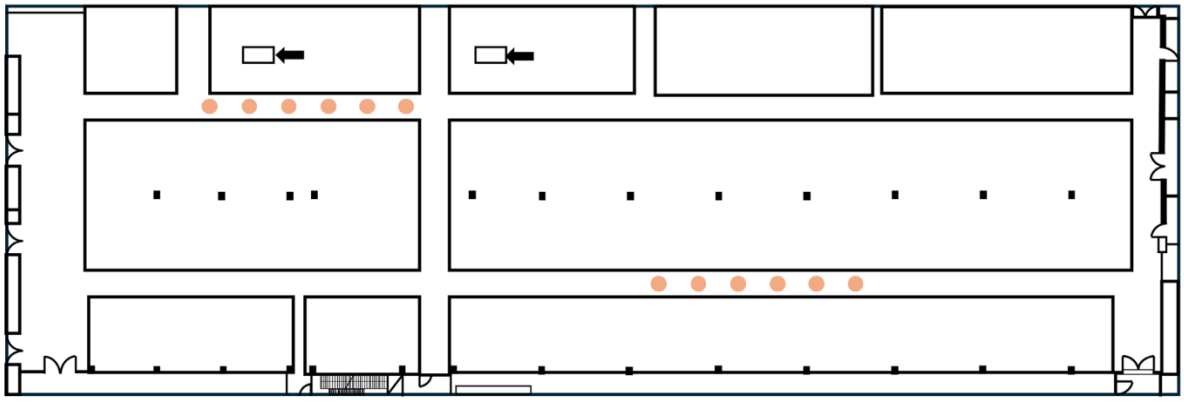

Figure 3-3: Distribution of the mmWave Devices across the Fraunhofer IPT Shopfloor.

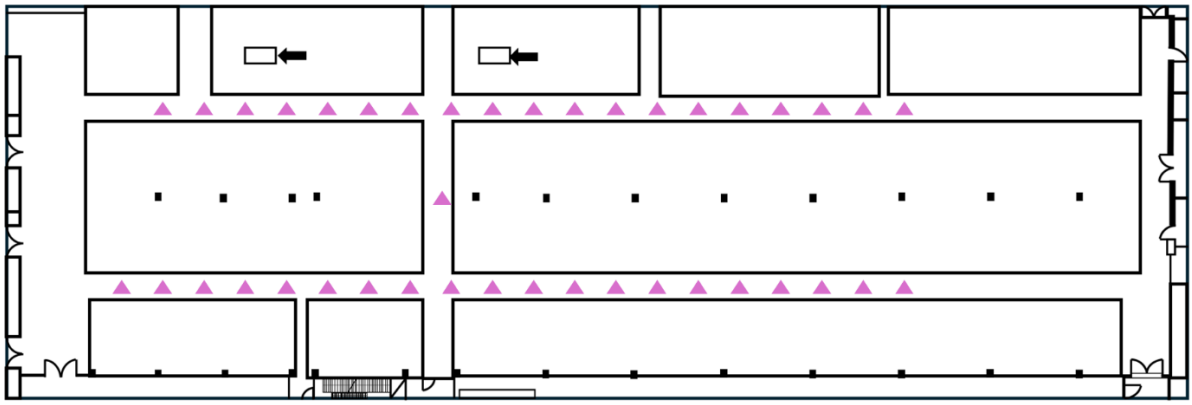

Figure 3-4: Distribution of the RedCap Devices across the Fraunhofer IPT shopfloor.

Furthermore, in-situ pictures of the measurement campaign at the Fraunhofer IPT shopfloor can be found in Figure 3-5, showing the device distribution and cabling of the ethernet control network.

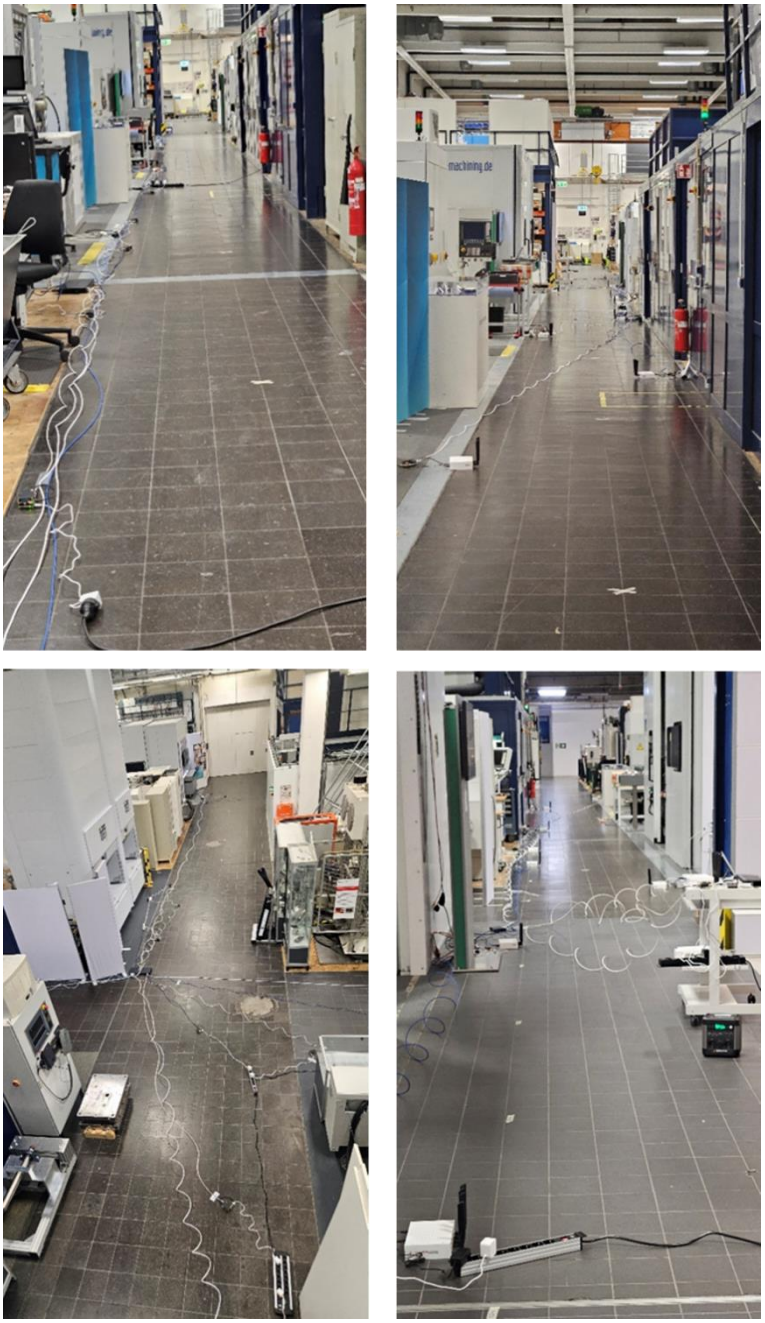

Figure 3-5: In-situ pictures of the measurement campaign

3.3.2 Results

In this subsection, the results of the different measurements are presented. It is important that not all measurements that were described above were carried out for every network feature for technological reasons.

Sub-6 GHz Measurement Results

For the midband, Time-to-Attach (TTA) measurements were carried out first. In an initial trial, all devices were attached sequentially to the 5G SA network. In a second measurement, the effect of 60 devices attaching in parallel was evaluated. The violin plot in Figure 3-6 shows the different distributions of the network attach times. In the sequential scenario, the mean TTA was 0.2 s lower. The parallel attachment of all 60 devices not only increased the mean TTA but also caused a wider statistical spread.

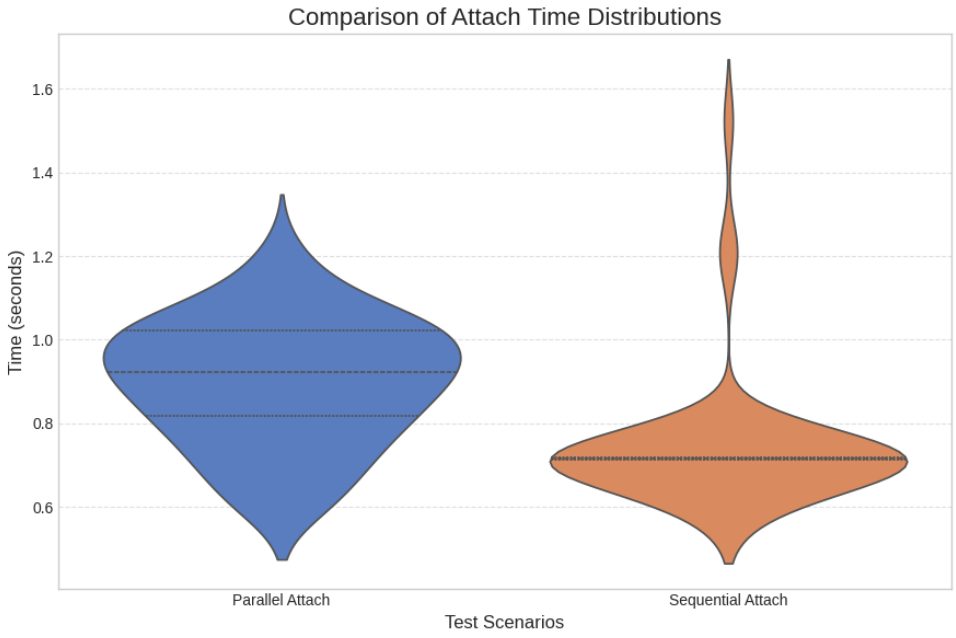

Figure 3-6: Violin Plot of TTA Measurements. Left: Parallel; Right: Sequential.

Another metric evaluated was the network's performance under simultaneous traffic load, which also provides an indication of the fairness of the 5G SA network. Figure 3-7 shows the timeseries and CDF (Cumulative Distribution Function) of the DL traffic for different numbers of devices. It should be noted that the traffic for a single device was capped at 250 Mbps due to hardware limitations.

The graph shows a high degree of fairness in the 5G SA network. Even when many devices receive traffic simultaneously, the DL throughput per device remains similar. Observed differences in DL throughput results can mostly be correlated with different RSRPs at the devices. As the number of devices increases, the throughput per device decreases linearly. The lower graph (CDF) additionally gives an indication of the fairness over different amounts of devices in the network.

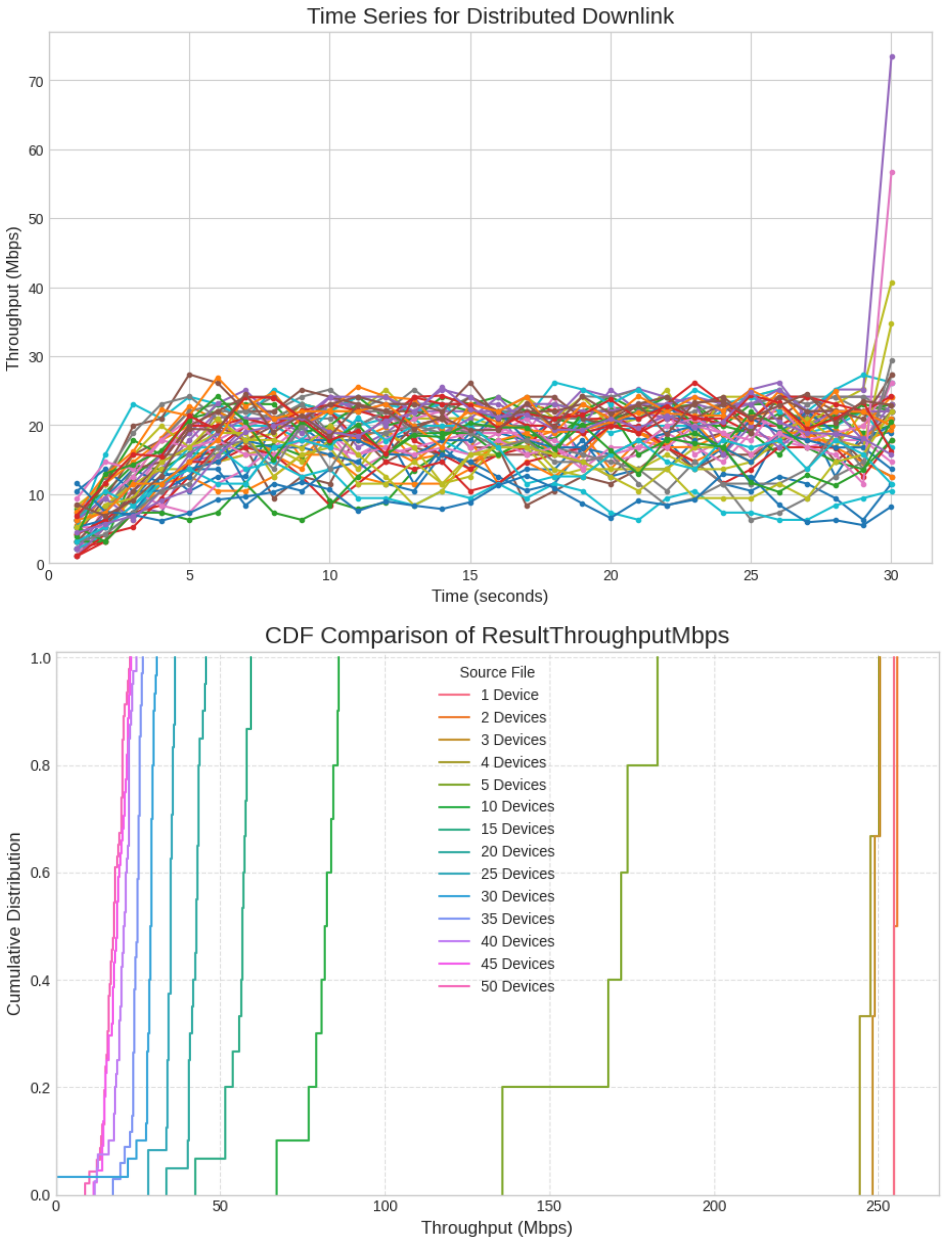

Figure 3-7: Timeseries and CDF of the DL

The same measurements were also conducted for the uplink (UL). Figure 3-8 shows the timeseries and CDF function of the UL throughput for the devices. In the UL throughput test, the mean throughput is also distributed fairly across all devices. However, the timeseries reveals that some devices experience an UL throughput of 0 Mbps for short periods. A possible reason for this could lie in a conflict between the TCP scheduling and the 5G SA network's own scheduler, leading to brief periods of packet loss.

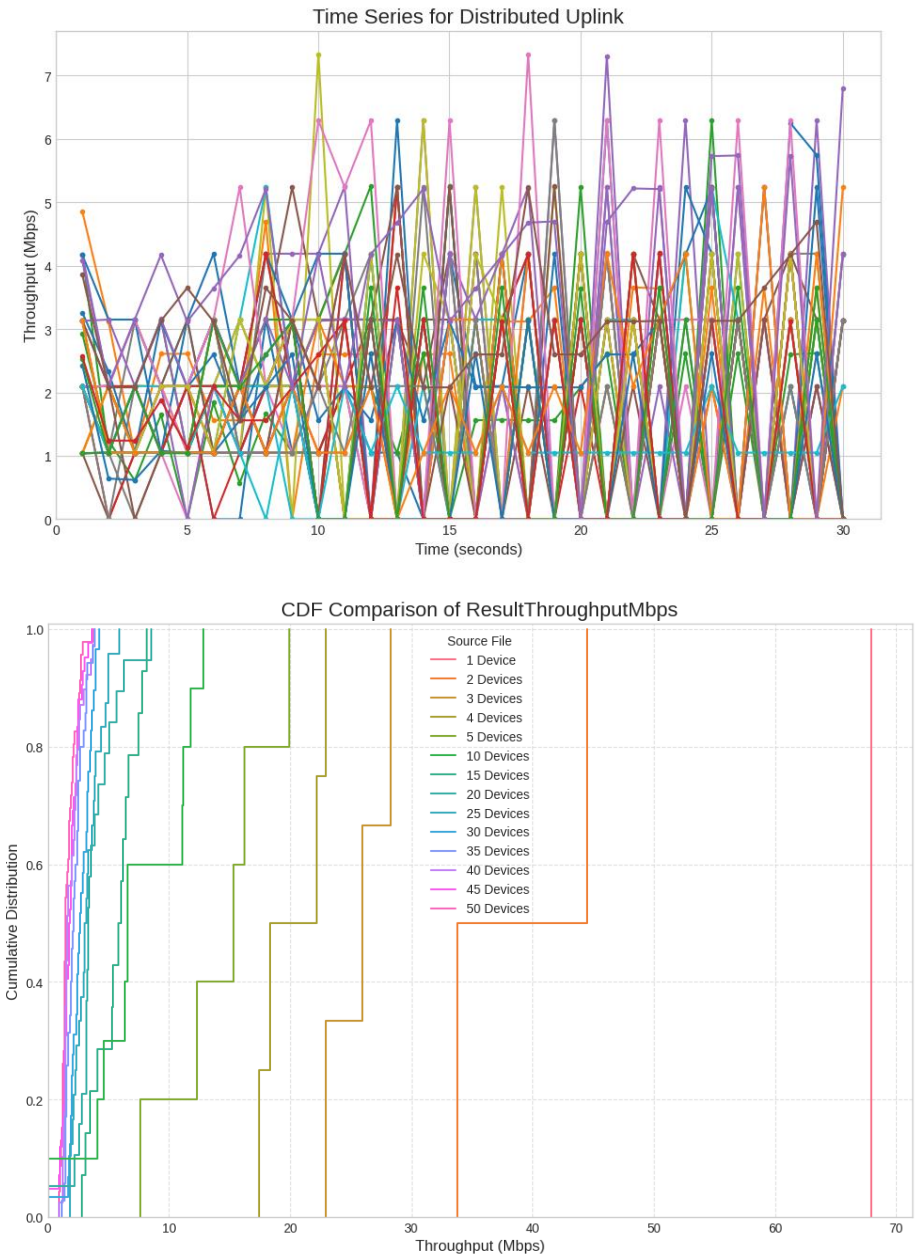

Figure 3-8: Timeseries and CDF Function of the UL

In Figure 3-9 the graphs correlatie the number of devices with the average throughput per device, resulting in a scaling graph of the system. It can be seen (blue line) in both DL and UL, that the average throughput per sensor decreases inversly proportional with the number of devices. Furthermore, the red line indicates the aggregated throughput of all devices. After the cell limit is reached, the agggregated throughput stays stationary.

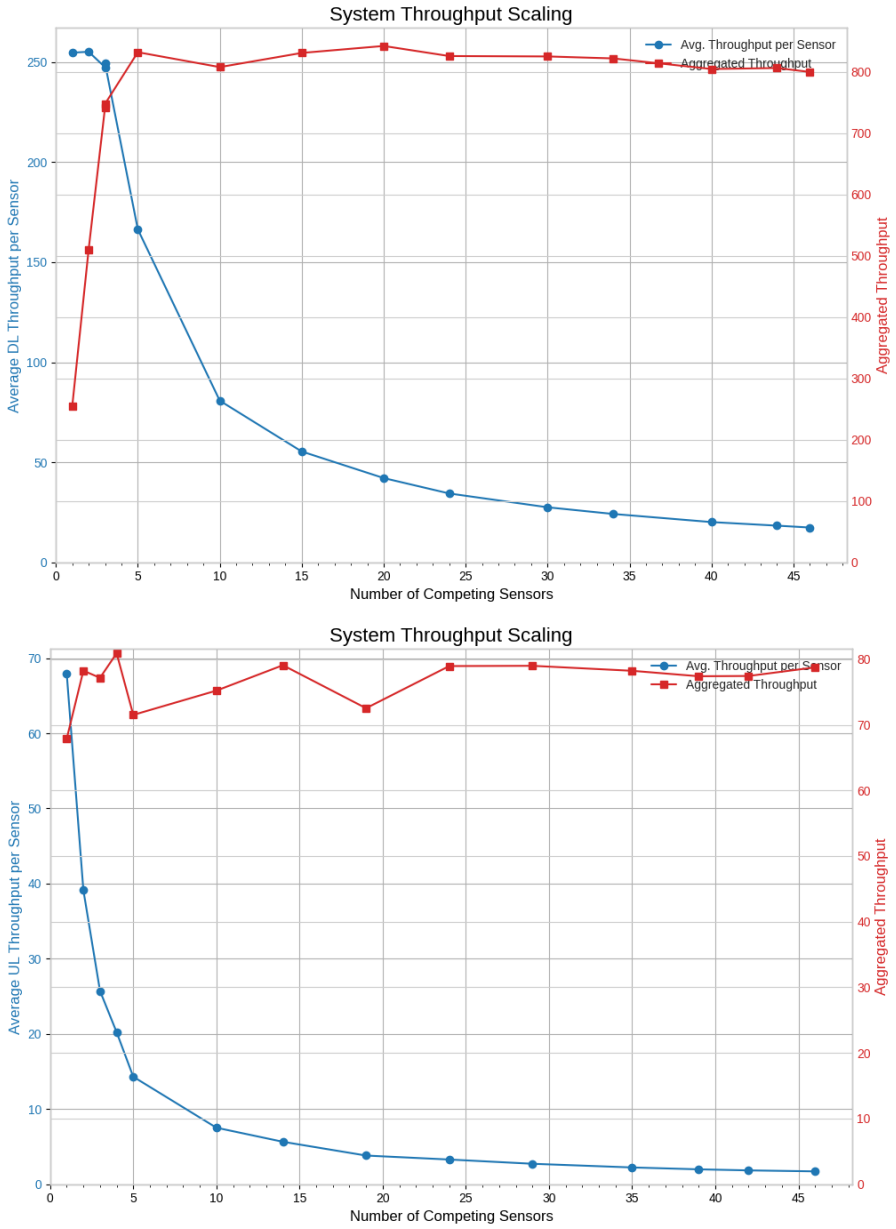

Figure 3-9: Scaling Graphs of the DL and UL

Additionally, a long-term stability analysis was conducted as shown in Figure 3-10. Each of the sensors was set to a fixed upload of 5 Mbps, resulting in an aggregated target throughput of 300 Mbps. This aggregated load led to an increased mean latency and jitter over all devices. With 300 Mbps, an overload of the cell in UL is targeted. The increasing latency is the effect of schedulers and network buffers.

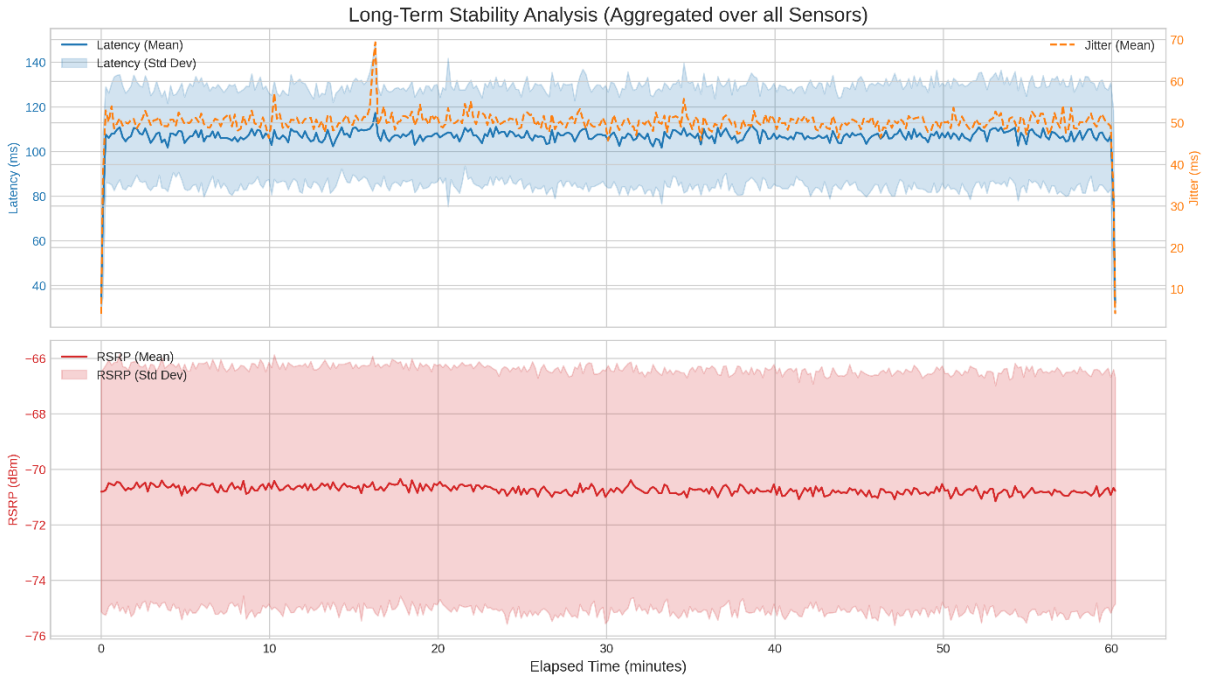

Figure 3-10: Long-term stability analysis with UL overload

mmWave Measurement Results

Also, for the mmWave network, the TTA measurements were conducted at first. As seen in Figure 3-11, the statistical spread for the parallel attach of all devices is slightly wider than for the sequential attach of all devices. Also, one outlier at 2.4 seconds can be seen in the parallel attach, indicating a failure followed by a second attempt to attach.

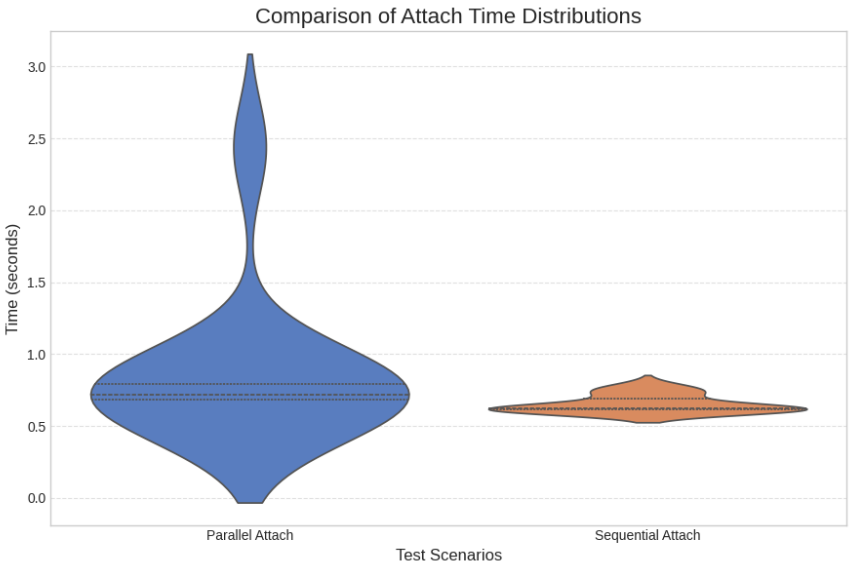

Figure 3-11: Time to Attach Test Sequential and Parallel

Subsequently the distributed DL throughput test was conducted. The timeseries of the mmWave downlink (Figure 3-12 reveals generally a high level of fairness. However, different throughput levels are visible at about 230 Mbps, 300 Mbps and 500 Mbps. These different levels of DL throughput are expected to be a result of the channel estimation of the 5G mmWave network, leading to the assignment of different Modulation and Coding Schemes (MCS).

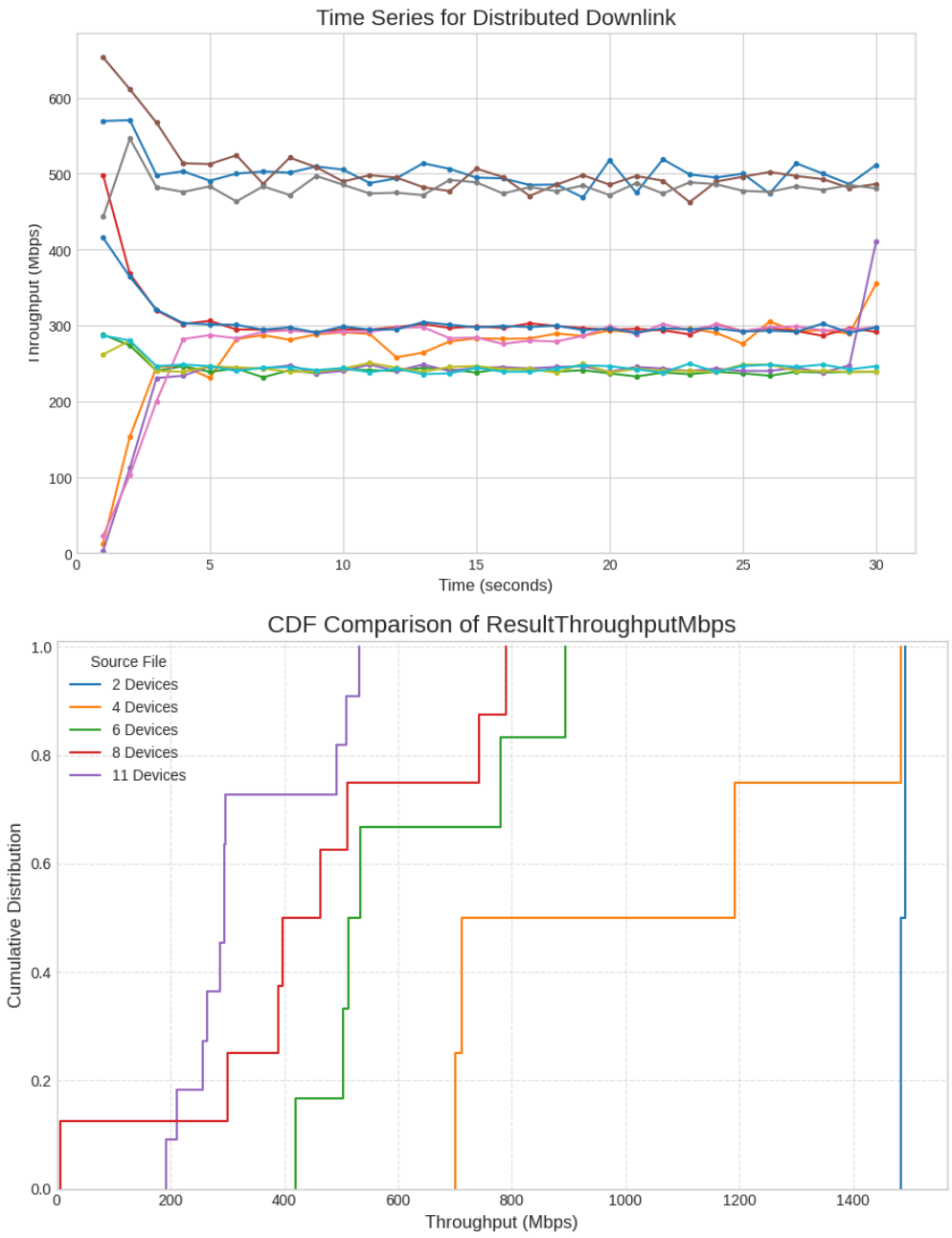

Figure 3-12: Timeseries and CDF of the mmWave Downlink.

As seen in Figure 3-13, the same behavior cannot be seen for the UL timeseries. The UL throughput of the mmWave devices is all at the same level. The CDF function confirms the fairness of the mmWave UL.

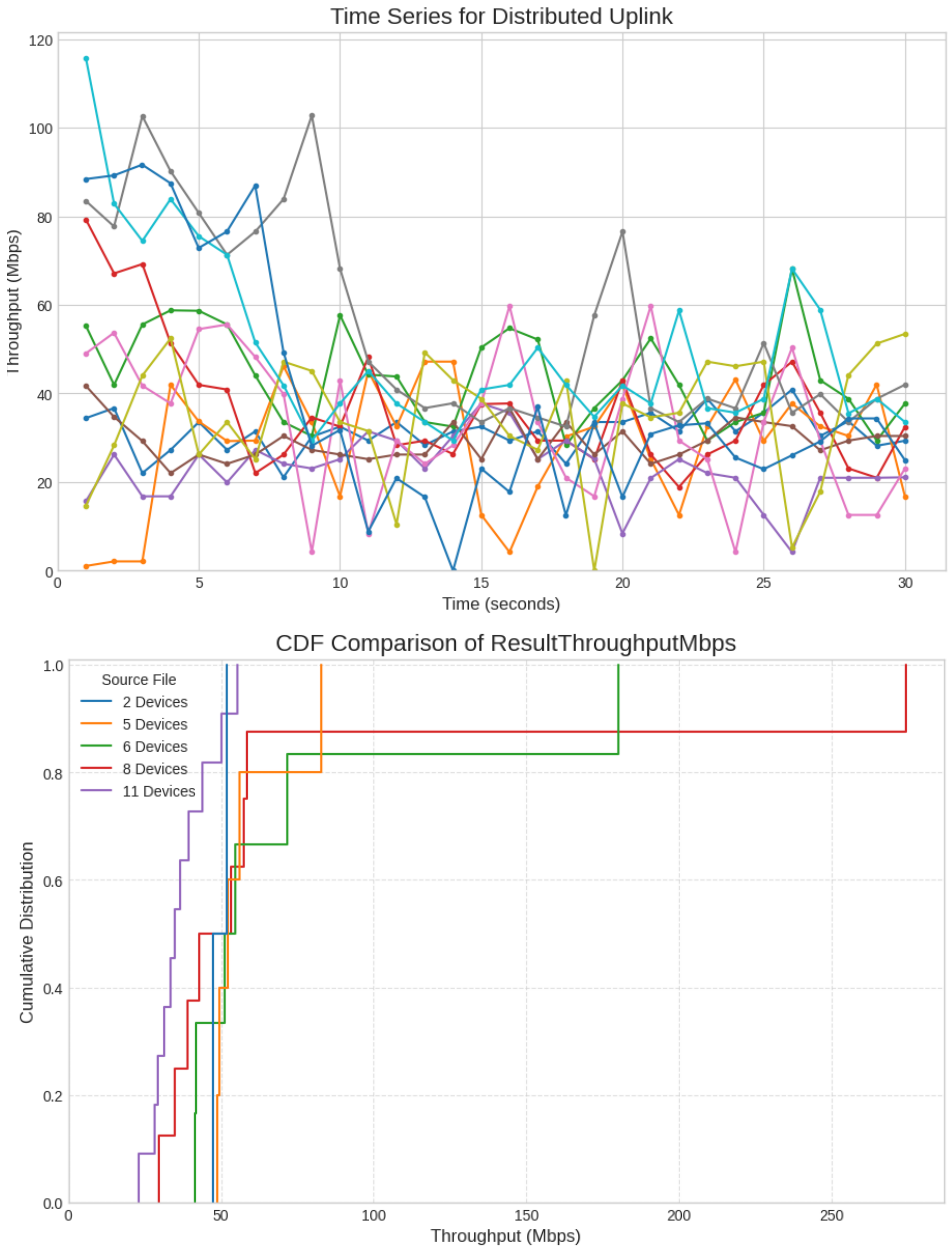

Figure 3-13: Timeseries and CDF of the mmWave Uplink.

Figure 3-14 shows the scaling graph of the mmWave DL and UL. Generally, similar behavior as in the previous sub 6 GHz measurements can be seen. An aggregated throughput of more than 4 Gbps was observed in the DL measurements. With an increasing number of devices, the throughput per device scales down according to the cell limitation.

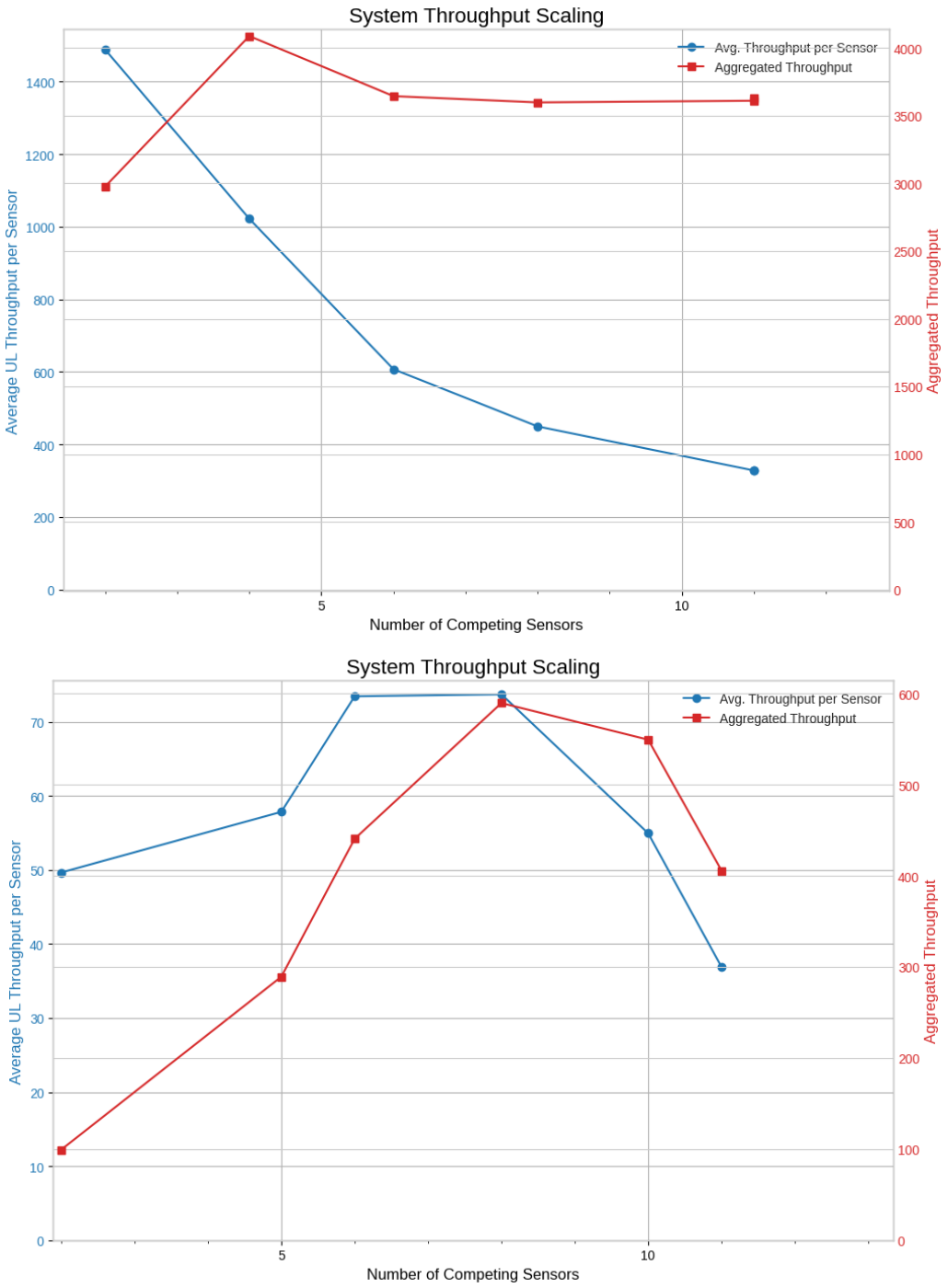

Figure 3-14: Scaling Graphs of the mmWave Measurements

A long-term test was also conducted during the mmWave measurements, plotted in Figure 3-15. Each device was loaded with a UL throughput of 15 Mbps, not reaching the cell limit. A very low RTT latency of 8ms was observed, combined with a mean jitter of less than 2 ms. Therefore, the system showed a very stable behavior under long-term load.

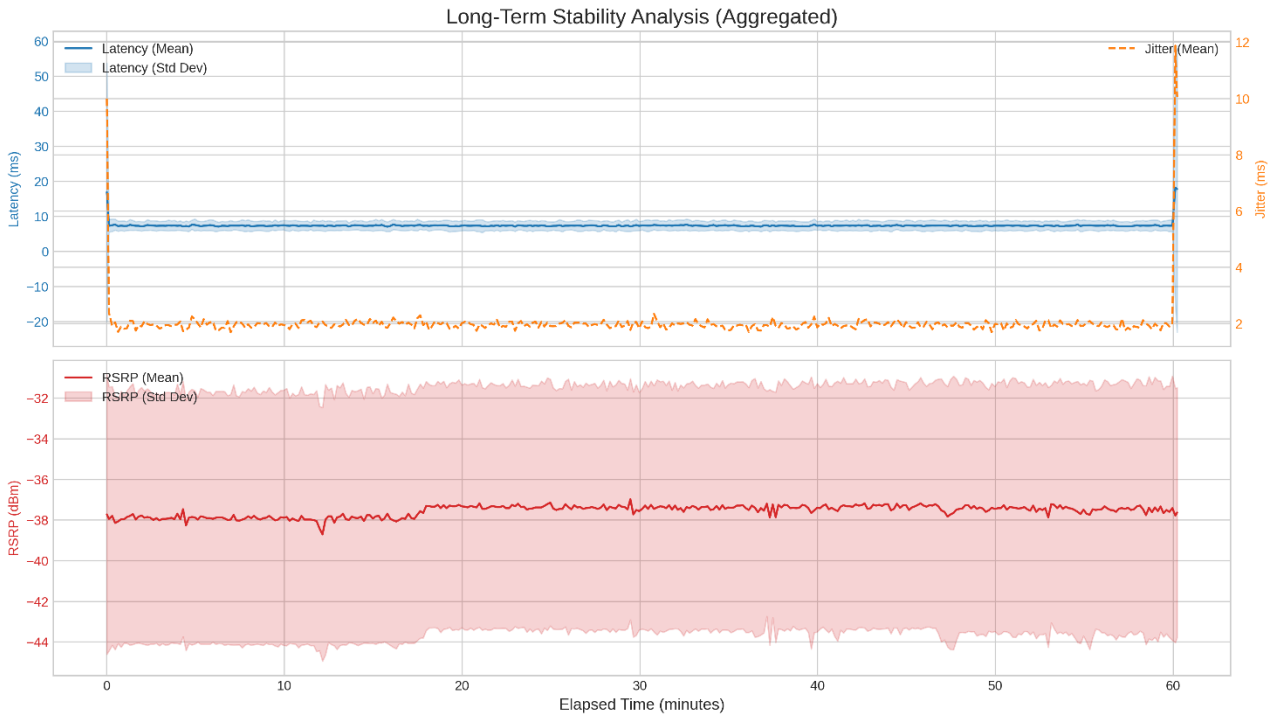

Figure 3-15: mmWave Longterm Test

RedCap Measurements

Lastly, the ReadCap measurements were conducted with 40 devices. During the test it was possible to attach all 40 devices to the network. However, the simultaneous communication of the devices was limited to 26 devices. More devices being active led to highly increased latencies resulting in timeouts. The reason for that is, that all Physical Resource Blocks (PRBs) were already distributed to the devices, leading to heavy congestion.

Because of these limitations, the measurements focused on the DL case. Figure 3-16 shows the DL timeseries and CDF function for 26 active RedCap devices. The timeseries reveals a high level of fairness among the devices. However, the throughput is varying heavily over the test duration. In some short intervals, some sensors also drop to 0 Mbps.

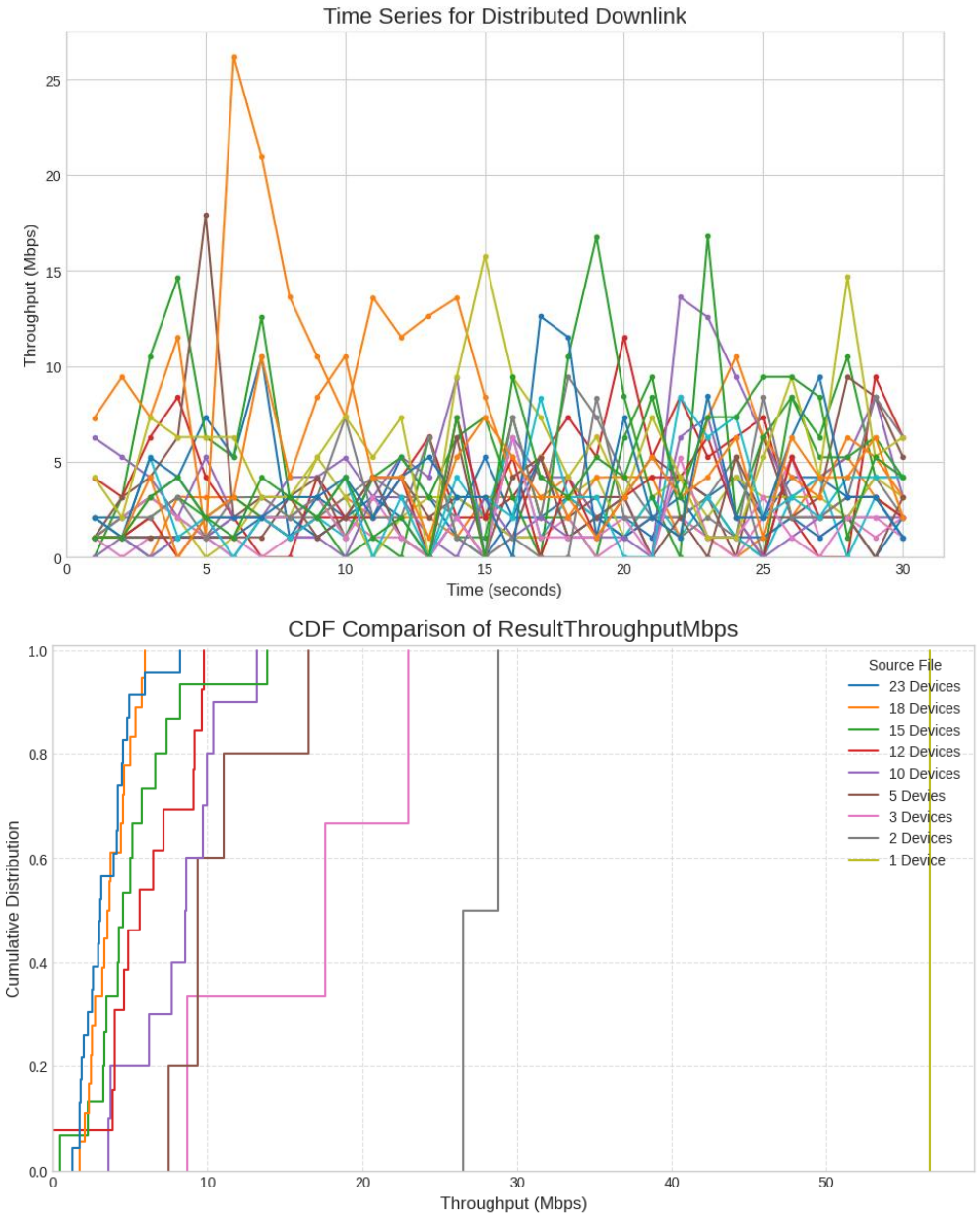

Figure 3-16: Timeseries and CDF for RedCap DL

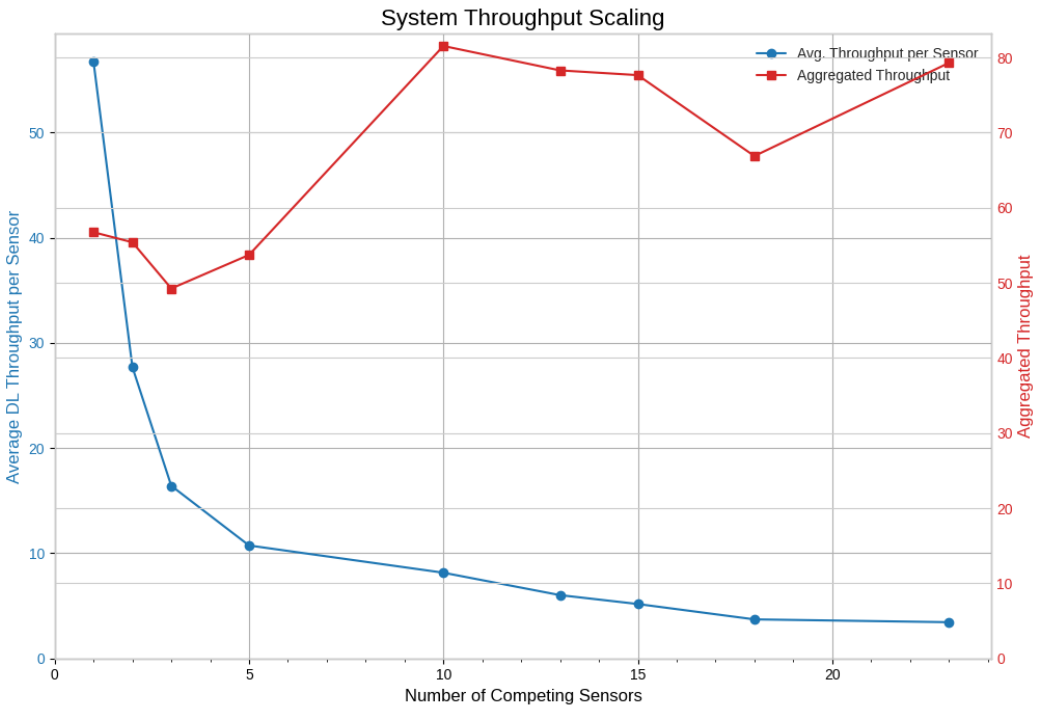

Figure 3-17: Scaling Graph of the Redcap Downlink

The scaling graph in Figure 3-17 again shows similar behavior as the other technologies. With an increasing number of devices, the aggregated cell limit is reached and the average DL throughput per sensor decreases. The aggregated DL throughput limit of RedCap cell was measured to be slightly above 80 Mbps.

3.4 Findings

The measurement campaign was concluded successfully, providing significant insights into the behavior of 5G networks across various technologies, including Sub-6 GHz, mmWave, and RedCap. A primary finding is the network's fair resource allocation, which distributes capacity evenly among active devices. Consequently, as the number of competing devices increases, the average throughput per device decreases, demonstrating predictable scaling behavior. Despite this effect, the network proved highly capable of managing a large number of devices effectively.

Furthermore, the investigation highlighted significant performance discrepancies between the different 5G technologies. The network demonstrated robust stability over extended periods, even when subjected to distributed load. Regarding connection latency, the attach time showed a slight, though not substantial, increase during scenarios with mass concurrent device attachments. It was observed, however, that the distribution of attach times became notably wider under these high-contention conditions compared to single-device attachments.

Based on these findings, further measurements are required to explore different network configurations. Future work should also encompass a wider range of test scenarios, such as the combined performance of mixed technologies operating concurrently and the impact of device mobility.

4 Learnings and outlook

4.1 Technical learnings

Uplink challenge

Use cases in industry have different requirements, compared to those of regular mobile communication users with eMBB characteristics. The most received comment is that more uplink bandwidth is needed, as many of the industrial use cases require big data transfers in the uplink direction, from UE to the network (edge), for further processing. Typical scenarios are video streams or LiDAR point clouds that require further processing to detect objects of relevance for the process. Solving the uplink challenge for industrial users, will be a clear enabler to further increase the user base. Solutions could be the introduction of more an dedicated spectrum, allowing more flexible use of existing spectrum.

Availability of devices

The availability of devices, useable in industrial environments, is still rather limited. While smartphones get the latest features and developments, and newest chipsets integrated very frequently, modules for industrial use lag behind or significant efforts must be made to create carrier boards that host the relevant 5G modules.

The selection of devices in midband is steadily increasing, now also with the RedCap devices being introduced into the market. European countries, such as Germany, have allowed mmWave spectrum to be requested for private use, but unfortunately the availability of modules and/or devices for the EU bands is still very limited.

Another challenging aspect in identifying suitable devices remains the form factor or feature set. The market to provide enterprise connectivity (Wireless WAN) is a driver in the device market. As such, this is a good evolution, but on the downside, it implies that most devices are WWAN routers that offer too many features, such as WiFi AP, internet-based management, firewalling, etc. This type of device is often too large for integration into robots or AGVs and consumes too much power due to the extensive feature sets.

NW technology

The migration towards 5G SA is progressing at a slow pace. Many mobile networks operators are rolling out 5G SA, but to realize good coverage across, significant investments are needed to make radio sites 5G SA capable. Without good SA coverage, not just in hotspot areas, the demand for, and availability of 5G SA capable devices lags.

3GPP has standardized interesting features for 5G and 5G advanced, but not all these features find their way to the end-users' groups at the same time. The features of interest to bigger user groups are typically available sooner, but unfortunately these features are not always useful for industrial scenarios.

Feature availability and network optimizations

As highlighted above, larger user groups drive the introduction of new functionality in many cases, to the disadvantage of smaller user groups such as the verticals addressed in TARGET-X. Industrial users would benefit from more balanced distribution of UL and DL bandwidth, or would even need more UL vs DL bandwidth, yet eMBB scenarios often prefer data consumption from the network to the UE.

Features such as 5GLAN and Ethernet PDUs have been standardized in 3GPP and are of great relevance when intending to use industrial protocols such as PROFINET, CC-Link over 5G. Unfortunately, there is still no mass market demand for this functionality and with that, no availability outside of prototype or niche developments.

4.2 Societal learnings

Cost of deployment

A concern that was frequently raised, for example when discussing with FSTP beneficiaries, is the cost of devices. A comparison with WiFi6 or WiFi7 technology is often made and used as an argument against 5G as the purchasing cost for devices is significantly lower than 5G devices. A fair comparison between the different wireless network technologies is difficult to realize as many of the differences require a deeper understanding of the underlying technology or become visible only when using large amounts of devices or when covering vast areas.

Learning curve

The learning curve of 5G technology is deemed steeper than for other wireless technologies.

Why 5G often feels harder than other technologies, such as WiFi:

- Architecture and scope: Wi-Fi is largely an access-layer technology (APs, controllers, SSIDs), while 5G spans RAN + a core network and often edge compute (MEC). That breadth adds complexity.
- Planning and RF: 5G (especially mmWave) demands different cell planning, propagation modelling, and more rigorous capacity planning than typical Wi-Fi deployments.
- Operational tooling and monitoring: 5G cores generate new KPIs and require expertise with 3GPP concepts (RRC states, SSB, RSRP/RSRQ, KPIs across RAN and core) and different debugging workflows.
- Regulation and spectrum: Depending on whether you use licensed or unlicensed bands, there are legal and operational differences to learn.

4.3 Outlook

The standardization of 6G is in full swing and the learnings from flagship projects, such as HEXA-X-II [36], are being considered.

The evolution towards wireless connectivity in all areas continues, and with that, the need for more bandwidth as the amount of data that needs to be exchanged is steadily increasing. The availability of more spectrum in future generations of mobile communications is key to meeting the ever-growing demand for bandwidth.

The interaction between networks and the applications that use the network resources is increasing. APIs, such as CAMARA, will continue to become more relevant and will expand. The communication flows between networks and applications are expected to become bidirectional, where it will also be possible for the future network generations to raise demands towards applications.

Industry relevant features are slowly finding their way into the expanding feature sets of mobile communications networks. This trend is expected to steadily continue as the acceptance and introduction of mobile communications in industry continues.

5 Conclusions

Work Package 6 (WP6) in the TARGET-X project focused on introducing and validating a set of modular “technology bricks” that are expected to be important for future generations of mobile communications. These technology bricks were selectively deployed into network segments where their expected benefits for performance, reliability, or functionality were greatest, so that their practical impact could be assessed in realistic settings.

Deliverable D6.5 provides a comprehensive, final collection of findings about these introduced elements. Where feasible, each technology was evaluated through dedicated empirical measurements that quantified performance improvements and operational effects; for components that were not measurable in isolation, the evaluations were performed by the project’s vertical-focused work packages, which assessed relevance and applicability for specific industry use cases.

Beyond per-technology evaluation, the project executed a large-scale trial to assess 5G (and newer generation) capabilities for industrial communication at scale, documenting system-level effectiveness, deployment considerations, and lessons learned for industrial IoT scenarios.

To capture user- and integrator-facing experience, WP6 also ran a questionnaire among work package leaders: this gathered first-hand insights about how 5G technologies were introduced, which integration or operational issues surfaced, and which pitfalls and mitigation strategies proved important. The questionnaire was conducted while the second round of FSTP projects were already in progress, allowing those ongoing initiatives’ learnings to be incorporated. In conclusion, Deliverable D6.5 synthesizes evidence that 5G — and research directions toward 6G — are relevant and valuable across the project’s verticals. While 5G remains the fifth generation of mobile communications and brings mature capabilities for enhanced mobile broadband (eMBB), it is just the first generation that is being widely applied and adapted for industrial IoT; together with early 6G concepts, these technologies form a strong foundation for moving toward more wireless, significant processes throughout the industrial ecosystem.

6 References

[1] M. Brochhaus, “D1.1: Forward looking use cases, their requirements and kpis/KVIs.” Available: https://target-x.eu/wp-content/uploads/2024/02/231231_TARGET-X_D1.1_Forward-looking-use-cases_final-version.pdf

[2] “TS 23.501: System architecture for the 5G System (5GS).” Available: https://portal.3gpp.org/desktopmodules/Specifications/SpecificationDetails.aspx?specificationId=3144. [Accessed: Sep. 11, 2025]

[3] “Ericsson Private 5G - Private network for your industry,” *ericsson.com*. Available: https://www.ericsson.com/en/private-networks/ericsson-private-5g. [Accessed: Aug. 30, 2025]

[4] “GStreamer: open source multimedia framework.” Available: https://gstreamer.freedesktop.org/. [Accessed: Sep. 11, 2025]

[5] “Ericsson Cradlepoint R1900,” *Ericsson*. Available: https://cradlepoint.com/product/endpoints/r1900-series/. [Accessed: Sep. 11, 2025]

[6] “TS 23.401: General Packet Radio Service (GPRS) enhancements for Evolved Universal Terrestrial Radio Access Network (E-UTRAN) access.” Available: https://portal.3gpp.org/desktopmodules/Specifications/SpecificationDetails.aspx?specificationId=849. [Accessed: Sep. 11, 2025]

[7] “TS 23.402: Architecture enhancements for non-3GPP accesses.” Available: https://portal.3gpp.org/desktopmodules/Specifications/SpecificationDetails.aspx?specificationId=850. [Accessed: Sep. 11, 2025]

[8] “How to Use Traffic Steering with Multi-PDN.” Available: https://customer.cradlepoint.com/s/article/How-to-Use-Traffic-Steering-with-Multi-PDN. [Accessed: Sep. 11, 2025]

[9] “D5.1: Roadmap for the 5G/6G empowered deconstruction robotic platform.” TARGET-X, 2023. Available: https://target-x.eu/wp-content/uploads/2023/10/TARGET-X_D5.1_Roadmap-for-the-5G-6G-empowered-deconstruction-robotic-platform.pdf

[10] “D2.3: Report on implementation of the wireless edge control robotics use-case.” TARGET-X, 2025. Available: https://target-x.eu/wp-content/uploads/2025/01/D2.3_Report-on-implementation-of-the-wireless-edge-control-robotics-use-caseM22_final.pdf

[11] “D6.2: Report on the deployment and testing of evolved features.” TARGET-X, 2024. Available: https://target-x.eu/wp-content/uploads/2024/05/D6.2-REPORT-ON-THE-DEPLOYMENT-AND-TESTING-OF-EVOLVED-FEATURES.pdf

[12] “Multi-Technology Platform - Fraunhofer IPT,” *Fraunhofer Institute for Production Technology IPT*. Available: https://www.ipt.fraunhofer.de/en/offer/special-machines/multi-technology-platform.html. [Accessed: Oct. 19, 2024]

[13] J. Biosca Caro *et al.*, “Empirical Performance Evaluation of 5G Millimeter Wave System for Industrial-Use Cases in Real Production Environment,” *Electronics*, vol. 14, no. 3, p. 607, Jan. 2025, doi: 10.3390/electronics14030607

[14] J. B. Caro *et al.*, "Empirical Study on 5G NR Cochannel Coexistence," *Electronics*, vol. 11, no. 11, p. 1676, Jan. 2022, doi: 10.3390/electronics11111676

[15] "ASUS NUC 14 Pro | NUCs | ASUS Global." Available: https://www.asus.com/displays-desktops/nucs/nuc-mini-pcs/asus-nuc-14-pro/. [Accessed: Aug. 30, 2025]

[16] Ansari, J. *et al.*, "5G enabled flexible lineless assembly systems with edge cloud controlled mobile robots," in *IEEE 33rd Annual International Symposium on Personal, Indoor and Mobile Radio Communications*, Kyoto, Japan, Sep. 2022.

[17] "OptiTrack - Motion Capture Systems," *OptiTrack*. Available: https://optitrack3.payloadcms.app/home. [Accessed: Aug. 30, 2025]

[18] "Prime^{x} 41 - In Depth," *OptiTrack*. Available: http://optitrack.com/cameras/primex-41/index.html. [Accessed: Aug. 30, 2025]

[19] "D4.3: Enhancement of Automotive Use Cases with 5G and Beyond." TARGET-X, 2025. Available: https://target-x.eu/wp-content/uploads/2025/04/TARGET-X-D4.3-v1.0-Final.pdf

[20] "TS 36.355: Evolved Universal Terrestrial Radio Access (E-UTRA); LTE Positioning Protocol (LPP)." Available: https://portal.3gpp.org/desktopmodules/Specifications/SpecificationDetails.aspx?specificationId=2441. [Accessed: Sep. 01, 2025]

[21] "TS 23.271: Functional stage 2 description of Location Services (LCS)." Available: https://portal.3gpp.org/desktopmodules/Specifications/SpecificationDetails.aspx?specificationId=834. [Accessed: Sep. 01, 2025]

[22] "EVK-F9P," *u-blox*, Dec. 01, 2022. Available: https://www.u-blox.com/en/product/evk-f9p. [Accessed: Aug. 30, 2025]

[23] P. E. Kehl *et al.*, "5G-TSN Integrated Prototype for Reliable Industrial Communication Using Frame Replication and Elimination for Reliability," *Electronics*, vol. 14, no. 4, p. 758, Jan. 2025, doi: 10.3390/electronics14040758

[24] "D2.5: Report on Working Demonstrators and Validation Implemented for 5G/6G Technologies in Manufacturing." TARGET-X, 2025.

[25] "TS 29.435: Service Enabler Architecture Layer for Verticals (SEAL); Network Slice Capability Enablement (NSCE) Server Services." Available: https://portal.3gpp.org/desktopmodules/Specifications/SpecificationDetails.aspx?specificationId=4230. [Accessed: Sep. 01, 2025]

[26] "TS 29.564: 5G System; User Plane Function Services; Stage 3." Available: https://portal.3gpp.org/desktopmodules/Specifications/SpecificationDetails.aspx?specificationId=3938. [Accessed: Sep. 01, 2025]

[27] "TS 29.572: 5G System; Location Management Services; Stage 3." Available: https://portal.3gpp.org/desktopmodules/Specifications/SpecificationDetails.aspx?specificationId=3407. [Accessed: Sep. 01, 2025]

[28] "TS 29.520: 5G System; Network Data Analytics Services; Stage 3." Available: https://portal.3gpp.org/desktopmodules/Specifications/SpecificationDetails.aspx?specificationId=3355. [Accessed: Sep. 01, 2025]

[29] "Quality on Demand – Camara Project." Available: https://camaraproject.org/quality-on-demand/. [Accessed: Aug. 30, 2025]

[30] "[OpenWrt Wiki] Welcome to the OpenWrt Project." Available: https://openwrt.org/. [Accessed: Sep. 02, 2025]

[31] "D6.3: Design and implementation of required submodels, exposures and interfaces." 2023. Available: https://target-x.eu/wp-content/uploads/2024/02/TARGET-X_D6.3_v1.0-Design-and-Implementation-of-Required-Submodels-Exposures-and-Interfaces.pdf

[32] "D6.4: DEVELOPMENT OF AAS INSTANCES AND REALIZING THE NETWORK/ASSET ORCHESTRATION." 2024. Available: https://target-x.eu/wp-content/uploads/2025/01/TARGET-X_D6.4_v1.1-Development-of-AAS-instances-and-realizing-the-Network-Asset-Orchestration.pdf

[33] "D3.4: Energy Data and Automation Architecture Report." TARGET-X, 2024. Available: https://target-x.eu/wp-content/uploads/2025/01/TARGET-X-D3.4-V1.0-Energy-data-and-automation-architecture-report.pdf

[34] "VILLASframework." Available: http://www.fein-aachen.org///projects/villas-framework/. [Accessed: Aug. 30, 2025]

[35] "RedCap: Expanding the 5G device ecosystem - Ericsson." Available: https://www.ericsson.com/en/reports-and-papers/white-papers/redcap-expanding-the-5g-device-ecosystem-for-consumers-and-industries. [Accessed: Aug. 30, 2025]

[36] "Hexa-X-II - European level 6G Flagship project." Available: https://hexa-x-ii.eu/. [Accessed: Aug. 30, 2025]